8-2003

Spectroscopic Examination of the Catalytic Decomposition of hydrogen Peroxide by a Copper (II) Complex of a Dissymmetric Schiff Base and an Imidazole Derivative.

John D. Davis Jr.
East Tennessee State University

Spectroscopic Examination of the Catalytic Decomposition of Hydrogen Peroxide by a Copper (II) Complex of a Dissymmetric Schiff Base and an Imidazole Derivative

---

A thesis

presented to

the faculty of the Department of Chemistry

East Tennessee State University

In partial fulfillment

Of the requirements for the degree

Master of Science in Chemistry

By

John D. Davis, Jr.

August 2003

Dr. Jeffrey G. Wardeska, PhD. Chair

Dr. Thomas T. Huang, PhD.

Dr. Ismail O. Kady, PhD.

Keywords: Copper (II) Complexes, Hydrogen Peroxide, Catalase, Catalyst

ABSTRACT

Spectroscopic Examination of the Catalytic Decomposition of Hydrogen Peroxide by a Copper (II) Complex of a Dissymmetric Schiff Base and an Imidazole Derivative

by

John D. Davis, Jr.

Previous studies involving copper (II) complexed with a dissymmetric Schiff base and imidazole derivatives had identified catalase activity of these complexes towards H_2O_2. Reactions such as this are of great interest due to the important role of copper-based complexes in biological systems. Our research has been conducted to add to the base of knowledge regarding the efforts of other researchers to investigate copper complexes that exhibit similar reactivity as copper-based proteins towards dioxygen. The copper complex chosen for this study contained a tri-dentate Schiff base adduct which, when complexed with an imidazole derivative, limited the manner in which peroxo adducts could bind while providing distinct spectral peaks which were used to conduct kinetic studies. Our results indicate a reaction mechanism by which the role of the complexed copper (II) ion is to activate the peroxo adduct for decomposition through reactions with other peroxide molecules, dioxygen, and water.

CONTENTS

LIST OF TABLES

Table Page

LIST OF FIGURES

Figure Page

CHAPTER 1

INTRODUCTION

The characterization and investigation of complexes of copper (II) with a dissymmetric Schiff base and its imidazole derivatives in previous studies have identified several intriguing properties of this family of compounds (*1*). One such property of these complexes was the observation of catalase activity towards the decomposition of hydrogen peroxide in aqueous ethanol solutions (*1*). Catalases are biological compounds that catalyze chemical reactions under biological conditions (i.e. low temperature, aqueous or lipid solvent systems, etc.). Catalase activity involves reactions of chemical compounds that mimic the reactivity of catalases in decomposition reactions. In the case of copper catalases that mediate the catalytic decomposition of hydrogen peroxide, a general overall balanced equation for this reaction would be:

$$2\ H_2O_2 \xrightarrow{\text{CuCatalase}} 2\ H_2O + O_2$$

The binding, activation, and metabolism of dioxygen (O_2) by copper ions in biological systems has spawned extensive research aimed towards deducing the fundamental chemistry involved in these reactions. It is generally accepted that the first step in the metabolism of dioxygen in copper-based systems is the reaction of dioxygen with a coordinated copper (I) ion to produce a copper (II) peroxo or superoxo intermediate (*2*). Many metalloproteins that contain copper sites and interact with dioxygen have been identified. Examples of these include hemocyanin, tyrosinase, and multicopper oxidases such as laccase, ascorbate oxidase, and ceruloplasm (*3*). These three multicopper oxidases are known to catalyze the 4-electron reduction of dioxygen to water (*4*).

In an effort to understand the fundamental aspects of the metabolism of dioxygen by copper-based proteins, an extensive amount of research has been conducted to identify, characterize, and investigate copper complexes that exhibit similar reactivity as these copper-based proteins towards dioxygen. Both mononuclear copper(II) – superoxide adducts (*5*) and peroxo-dicopper(II) complexes have been synthesized, characterized, and studied. In the case of peroxo-copper (II) complexes, four classes of compounds have been isolated at low temperatures (-80^{o} C) in solution via the reaction of dioxygen with the appropriate copper (I) complexes. Figure 1 provides these four structures along with a description of the key characteristics of their spectra. (*6*)

A couple of key observations have been made regarding reactions of copper complexes and dioxygen. One researcher stated, "In every case thus far examined, the binding sites of all Cu (II) proteins contribute nitrogenous ligands to the metal ion" (*7*). More specifically, the research conducted to date has indicated that the predominantly reactive species were complexes in which two nitrogen atoms were directly coordinated to the copper ion (*8*).

The second key observation is that the nature and number of ligands coordinated to the copper ion plays a critical role both the kinetics and mechanisms of reactions. Depending on the nature of the ligands and the overall stereochemistry of the copper complex, both copper (I) and copper (II) oxidation states have been identified as having a role in the decomposition of the peroxo-copper (II) intermediates. One researcher has postulated a significant contribution of a peroxo-copper (III) resonance form in this reaction (*9*). Copper (II) complexes typically show a five-coordinate square pyramidal to distorted trigonal bipyramidal geometry with the geometry largely determined by the

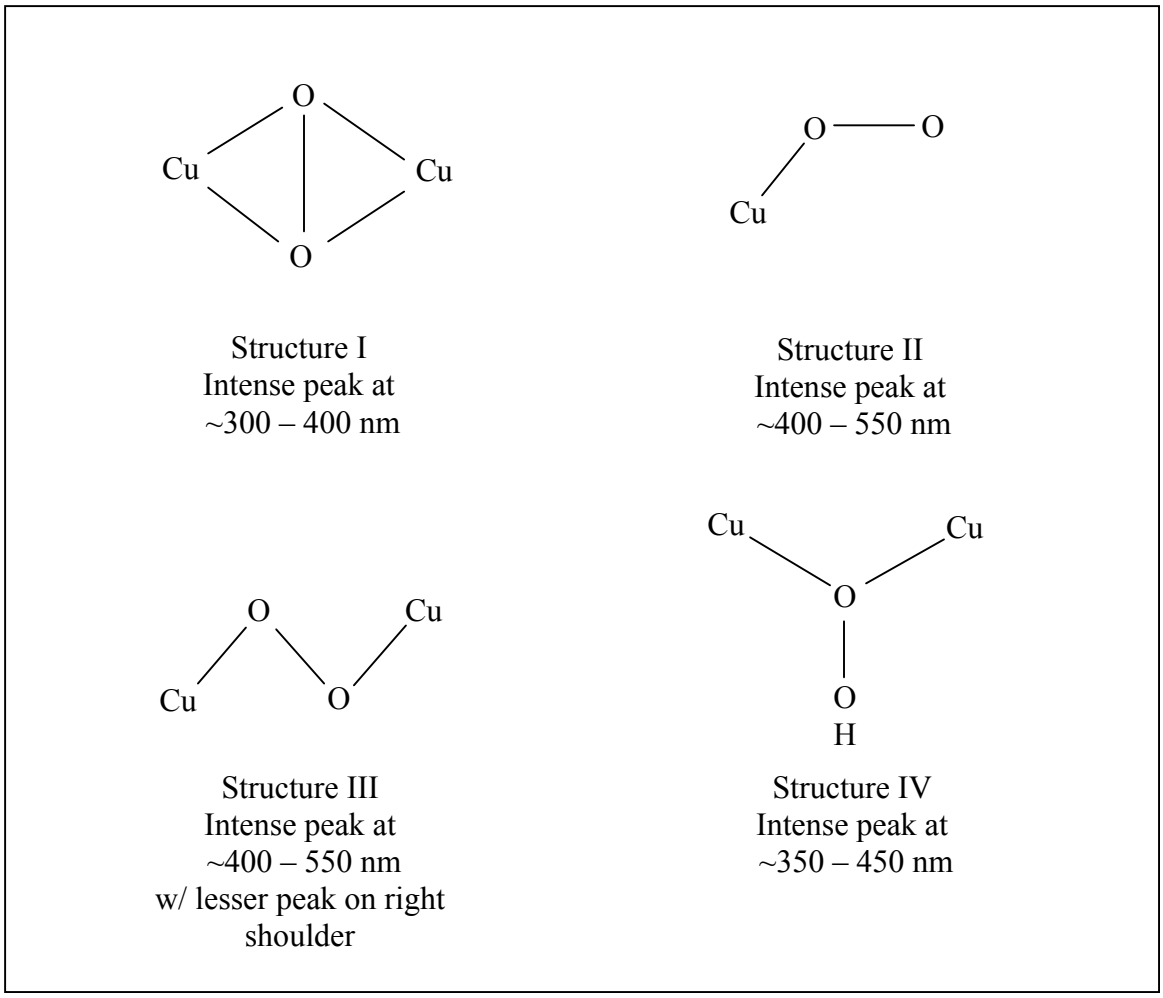

Figure 1: Four Classes of Peroxy-Copper(II) Complexes (*6*)

size, number, and nature of coordinated ligands. Copper (II) complexes exhibit spectral peaks in the range of ~500 – 600 nm that correspond to d-d transitions. Since d-d transitions are not possible in d^{10} metals, copper (I) complexes do not have spectral peaks in the 500 – 600 nm range. Another method for determining the oxidation state of copper is the use of 2,2'-biquinoline. Biquinoline reacts with Cu(I) ions to produce a pink-colored complex while solutions having Cu(II) ions exhibit no color change (*9*).

Changes in ligand size have been demonstrated to change the reaction rates of catalytic reactions of copper complexes (*10*) and in the case of peroxo complexes, the

number of coordinated ligands plays a role in the orientation of the peroxo oxygen atoms in dimeric copper (II) complexes. If three or fewer coordination sites are occupied, the peroxo prefers to bind in a "side-on" orientation with both oxygen atoms coordinated to both copper ions. If four sites are occupied, binding will occur in one of two possible "end-on" orientations. In one case, each oxygen atom will coordinate with separate copper ions. In the other case, both copper ions will coordinate with one oxygen atom while the other oxygen atom retains its proton (*4*).

Imidazole groups play an important role in dioxygen metabolism when copper is complexed by histidine-containing peptides (*11*). Imidazole is a five-membered nitrogen heterocycle and is an ubiquitous ligand in biological systems. It coordinates to transition metals such as copper via one of the two nitrogen atoms residing in the five-membered chain. It is present in proteins as part of the amino acid histidine side-chain, in nucleic acid structures as part of the purine ring of adenine and guanine, and as benzimidazole in the vitamin B-12 coenzyme (*12*).

Our research has been conducted to add to the basic knowledge regarding the effort to identify, characterize, and investigate copper complexes that exhibit similar reactivity as these copper-based proteins towards dioxygen. Most all of the research in this area has involved adding dioxygen to copper(I) complexes and studying the reactions of dioxygen with copper ions as it progresses through the various peroxy and superoxy forms ultimately to form water and hydroxide. The focus of this research has been the study of peroxy-copper reactions. Our research has expanded the reactions studied to include the investigation of peroxy-peroxy disproportionation reactions that are initiated by the involvement of copper(II) complexes. Hydrogen peroxide has the characteristic of

having thermodynamically favorable reactions in which the peroxide species could serve as both the oxidizing and reducing agent in a redox reaction in a disproportionation reaction. The following two half-cell reactions demonstrate this property for near physiological conditions, i.e., pH ~ 7:

$$HO_2^- + H_2O + 2e^- \leftrightarrow 3\ OH^- \text{ ; -0.828 V , and}$$

$$HO_2^- + OH^- \leftrightarrow O_2 + H_2O + 2e^- \text{ ; 0.076 V}$$

The overall balanced equation for this disproportionation reaction is:

$$2\ HO_2^- \leftrightarrow O_2 + 2\ OH^-$$

The copper complex chosen for this study, $[Cu(II)SalPAHP]_2 \cdot H_2O$, contains a three-coordinate Schiff base adduct resulting from the reaction between salicylaldehyde (Sal) and (*1S,2S*)-$(+)_D$-1-phenyl-2-amino-1,3-propanediol (PAHP), which, when complexed with an imidazole derivative, limits the available coordination sites for peroxo binding to one. This forces the peroxo moiety to bind in an "end-on" orientation. Figure 2 depicts the synthesis of the Schiff base and Figure 3 depicts the resulting dimeric $[Cu(II)SalPAHP]_2 \cdot H_2O$ complex when the Schiff base is reacted with copper(II) ions.

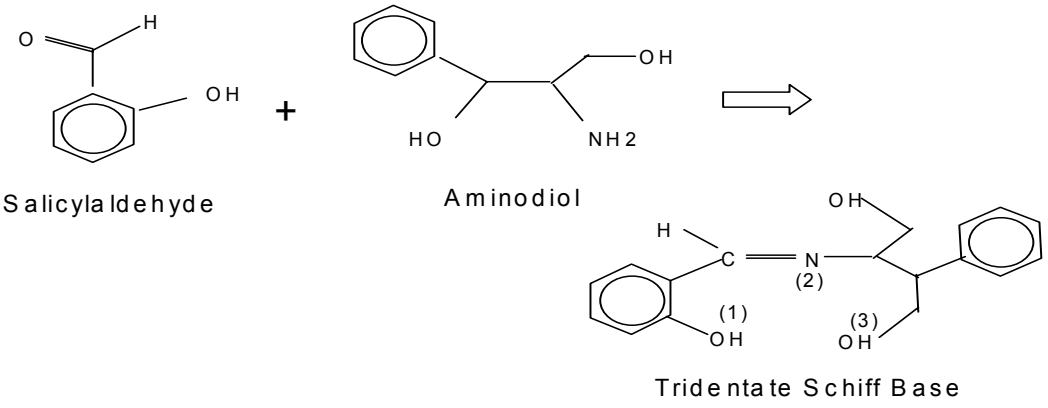

Figure 2: Synthesis of the Schiff Base

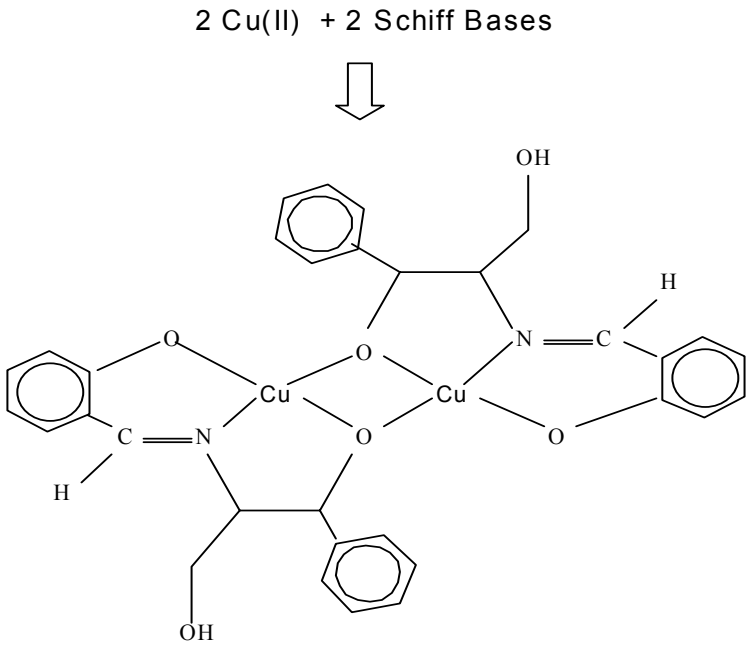

Figure 3: Reaction of Copper(II) Acetate and Schiff Base to form $[Cu(II)SalPAHP]_2 \cdot H_2O$

One of the coordination sites for the Schiff base is a nitrogen atom. This, coupled with the nitrogen coordination atom in the imidazole ring, provides the optimal number of two coordinated nitrogen atoms for copper catalase reactivity. The use of an imidazole derivative is not only appropriate due to the presence of imidazoles in biological systems, it also provides flexibility in the design of the complex. Many imidazole derivatives are commercially available with a wide variety of substituents. This family of compounds provides a useful tool for investigating the effect of subtle changes in ligands on the reactivity of the copper ions.

While several imidazole derivatives were initially tested, research centered almost exclusively on 2-methylimidazole. Figure 4 shows a representation of the Cu(II)SalPAHP·2-MeIm complex used for this study. This imidazole derivative was

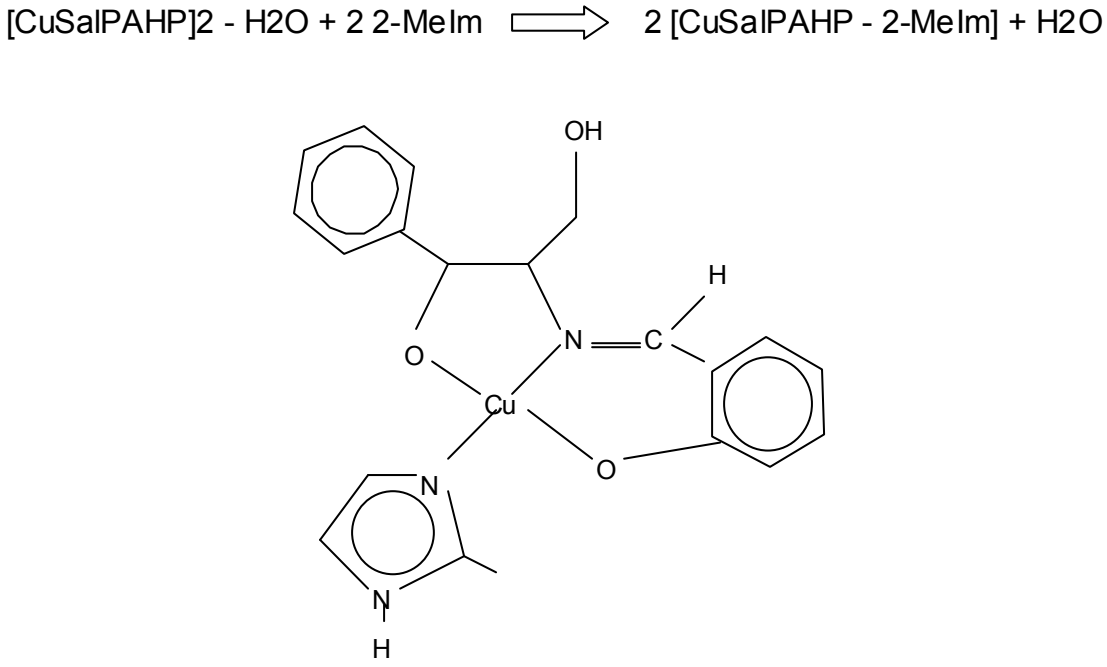

Figure 4: Reaction of $[Cu(II)SalPAHP]_2 \cdot H_2O$ Dimer with 2-Methylimidazole to form Cu(II)SalPAHP·2-MeIm

selected due to its stability in relatively high concentrations of hydrogen peroxide, the intensity of the spectral peaks of peroxo intermediates, and the resolution of individual peaks. A kinetic study was conducted on this copper (II) complex in order to propose a reaction mechanism for its catalytic decomposition of hydrogen peroxide. The progress of the reaction and the measurement of kinetic initial rates were accomplished via electron absorption spectroscopy.

CHAPTER 2

EXPERIMENTAL METHODS

Instruments, Glassware, and Miscellaneous Materials

The following instruments, glassware, software, and miscellaneous materials were used: Cary 14 UV/Vis/IR spectrometer, Sartoris laboratory balance, Jandel Scientific TableCurve, Microsoft Excel, 500 uL glass syringe, 22 gauge syringe needles, 50 mL volumetric flasks, 5 mL serological glass pipettes (graduated in 0.01 mL increments), 4 mL quartz crystal cuvettes, and miscellaneous laboratory glassware such as beakers, sample bottles, and graduated cylinders.

Reagent Grade Stock Chemicals

Reagent grade salicylaldehyde (Sal), (*1S,2S*)-$(+)_D$-1-phenyl-2-amino-1,3-propanediol (PAHPH), copper(II) acetate, imidazole (Im), 4-nitroimidazole (4-NIm), 2-methylimidazole (2-MeIm), 4-methylimidazole (4-MeIm), ethanol (absolute), 2,2'-biquinoline, and deionized water were used for testing.

Commercially prepared 0.9 M hydrogen peroxide solution (3%, USP grade) was used for testing.

Experimental Approach

Previous studies involving reactions of Cu(II)SalPAHP·Im with hydrogen peroxide had shown that the progress of the catalytic decomposition of the peroxide by the copper complex could be tracked through the formation of a spectrally active intermediate (peak at 440 nm). (1) A series of preliminary qualitative tests were performed in order to define the optimum reagents ranges for conducting a kinetics study of this system.

The tests involved the use of various concentrations of $[Cu(II)SalPAHP]_2 \cdot H_2O$, imidazole derivative, and initial hydrogen peroxide levels. In addition to varying the concentration of imidazole derivatives, four different imidazole derivatives were evaluated: imidazole (Im), 4-nitroimidazole (4-NIm), 2-methylimidazole (2-MeIm), and 4-methylimidazole (4-MeIm).

Based on these qualitative tests, the following conditions were selected for the kinetic study:

1. 2-Methylimidazole (2-MeIM) was selected as the imidazole derivative;
2. 2-MeIm concentration range = 0.001 – 0.005 M;
3. $[Cu(II)SalPAHP]_2 \cdot H_2O$ concentrations = 0.0001, 0.0002, and 0.0003 M;
4. Hydrogen peroxide initial concentration range = 0.00015 – 0.0025 M; and
5. Solvent was a 60/40 mixture of ethanol and deionized water.

Kinetics Study

A kinetics study was performed in order to attempt to deduce to the mechanism by which Cu(II)SalPAHP·2-MeIm catalytically decomposes hydrogen peroxide. Due to the formation of a second peak after about one minute, the kinetics study was performed by estimating the initial reaction rate for the first 30 seconds of the reaction. The initial rates were estimated via a previously described mathematical approach using absorbance (D) versus time (T) plots. (13, 14, 15) In this approach, absorbance versus time plots were fit to the polynomial equation:

$$D = a + bT + cT^2 + dT^3 + \ldots.$$

The first derivative of this expression is:

$$dD/dT = b + 2cT + 3dT^2 + \ldots.$$

And at T = 0, dD/dT = b

Thus "b" provides a good estimate of the initial rate of a reaction. Absorbance versus time plots were developed from the Cary 14 strip-charts for each kinetics test and fit to the polynomial equation using TableCurve software.

The following steps were followed for each kinetics test. A volume of 3.0 mL of Cu(II)SalPAHP·2-MeIm solution was pipetted into a 4 mL quartz crystal cuvette. The cuvette was placed in the Cary 14. The desired volume of pre-diluted hydrogen peroxide solution (0.05 – 0.25 mL) was added to the cuvette using the glass syringe. These volumes were selected to keep the dilution of the contents of the cuvette to less than 10%. The contents of the cuvette were stirred with the syringe for 5 seconds. The spectrometer chart was started after 10 seconds of total elapsed time with the wavelength fixed at 445 nm. The first 60 seconds of the reaction was charted. A time period of 60 seconds was chosen based on the observation in the preliminary qualitative tests of the appearance of the second intermediate peak. It was theorized that using some time interval of less than 60 seconds would minimize the contribution of the formation of the second intermediate to the initial rate attributed to the intermediate being studied at 445 nm.

CHAPTER 3

RESULTS

Preparation of Cu(II)SalPAHP·2-MeIm

The detailed synthesis of $[Cu(II)SalPAHP]_2 \cdot H_2O$ has been previously described (*1*). The $[Cu(II)SalPAHP]_2 \cdot H_2O$ used for this study was prepared by this method. In general, salicylaldehyde is reacted with (*1S,2S*)-$(+)_D$ 1-phenyl-2-amino-1,3-propanediol under reflux in ethanol to prepare the Schiff base SalPAHP. Once recrystalized and isolated, a yellow crystalline product is obtained. Figure 2 depicts the synthesis of the Schiff base.

The dimeric copper complex is obtained from the reaction of an aqueous solution of copper(II) acetate monohydrate with an ethanolic solution SalPAHP. The resulting green product is filtered, re-dissolved in ethanol, and precipitated by addition of water. The resulting $[Cu(II)SalPAHP]_2 \cdot H_2O$ has been well characterized and has been assigned the CAS Registry No. 80327-02-2. (1) Figure 3 depicts the resulting dimeric $[Cu(II)SalPAHP]_2 \cdot H_2O$ complex.

Imidazole derivatives of this complex were prepared by adding stoichiometric excesses of imidazole derivative to the dimeric $[Cu(II)SalPAHP]_2 \cdot H_2O$ in ethanol or in mixtures of ethanol and deionized water to form solutions of the monomeric Cu(II)SalPAHP·Im complex. For this study, mixtures of 60% ethanol and 40% deionized water were typically used. Tests using ethanol only were also performed. Typically, the $[Cu(II)SalPAHP]_2 \cdot H_2O$ was first dissolved in ethanol only. A bright Kelly-green solution was obtained. As the imidazole derivative was added and allowed to stand, a purplish-bluish solution formed. Aliquots of this solution were used for testing.

Preparation of "Active" Cu(II)SalPAHP·2-MeIm

Initially, the active form of the copper complex was prepared by synthesizing the Cu(II)SalPAHP·2-MeIm in the presence of water to produce the greenish-blue species described below and testing the samples before the greenish-blue color had decayed away to form the final purplish-blue color. Samples were typically used 2 – 3 hours after 2_MeIm addition. Most of the tests were performed using samples prepared in this manner.

Due to the striking similarity between the spectra from samples of the active species as prepared above to the spectra of non-active samples that had been dosed with peroxide and allowed to react for about 2 hours, it was theorized that the two species were actually the same.

This theory was tested by re-dosing several samples that had been treated with peroxide and allowed to react for 2 hours. Absorbance versus time plots were collected for these tests and compared to those collected from active samples prepared by synthesizing the copper complex in the presence of water. The spectra from these two differently prepared active samples seemed to be the same both in the appearance of the plots and in the initial rates that were estimated.

Fairly reproducible were obtained despite the somewhat subjective nature involve in the preparation of these samples.

Preliminary Qualitative Tests

Qualitative preliminary tests were performed in order to determine the optimum reagents ranges for the kinetics tests and for selecting the imidazole derivative to be used in the kinetics testing. Several key observations were made during these initial investigations. The first was that the use of too high of an initial hydrogen peroxide dosage would cause in irreversible reaction in which the copper was precipitated. A yellowish-orange precipitate was formed. No attempt was made in this project to characterize this precipitant. The levels of peroxide that would lead to this undesired reaction were not only dictated by the concentration of copper complex but also by the level of imidazole derivative present in the sample.

It was observed that increasing the levels of imidazole while keeping both copper and initial peroxide concentrations constant initially led to slightly higher reaction rates, reached a maximum rate, and then progressively slowed the overall reaction of the peroxide decomposition reaction as higher levels of imidazole were used. If insufficient levels of imidazole derivative were present, the undesired copper precipitation reaction would predominate when peroxide was added.

Other interesting observations resulted from the testing of four different imidazole derivatives. The four derivatives tested were: imidazole, 4-nitroimidazole, 4-methylimidazole, and 2-methylimidazole. The copper complex formed with 4-nitroimidazole was not stable. A reaction similar to the one that occurred when too much peroxide was added was observed. The other three derivatives formed clear greenish-blue solutions that gradually (over about an 8-hour time period) changed into purplish-blue solutions that remained stable over indefinite periods of time provided the solutions

were contained in tightly capped bottles to prevent the evaporation of the ethanol. It was interesting to note that if the Cu(II)SalPAHP·ImD (where "ImD" denotes generic imidazole derivative) complexes were prepared in ethanol only, or if the reagents were first dissolved in ethanol and then the deionized water was added, the solutions immediately became the final purplish-blue hue without going through the time-period in which the greenish-blue color grew in and subsequently decayed away. The pH of these solutions were ~7.9. It was observed that there was not a noticeable change in pH during the reaction of the Cu(II)SalPAHP·ImD complexes with peroxide.

Solutions of the three stable Cu(II)SalPAHP·ImD complexes that contained the same concentrations of copper and imidazole were tested with the same initial dosages of peroxide in order to observe the differences in performance for each imidazole derivative. The solution containing 2-MeIm yielded the most intense spectra and qualitatively seemed to be able to tolerate higher initial dosages of peroxide than the other two derivatives. Careful review of spectra obtained from the preliminary tests revealed that there was a second intermediate spectral peak at ~420 nm in addition to the reported peak at ~440 nm. This peak was difficult to detect due to its proximity to the peak at 440 nm and that the 420 peak started growing in about 1 minute later than the 440 nm peak. This second peak was most clearly seen when 2-MeIm was used. For 2-MeIm, the first intermediate peak was at 445 nm and the second peak was at 418 nm. Figure 5 provides a series of spectra clearly showing the presence of the two peaks and the order at which they appear. Changes in the shapes of the peaks for solutions containing Im and 2-MeIm indicated the presence of this second intermediate; however these two peaks could not be resolved for these samples. Due to the intensity of the intermediates peaks for solutions

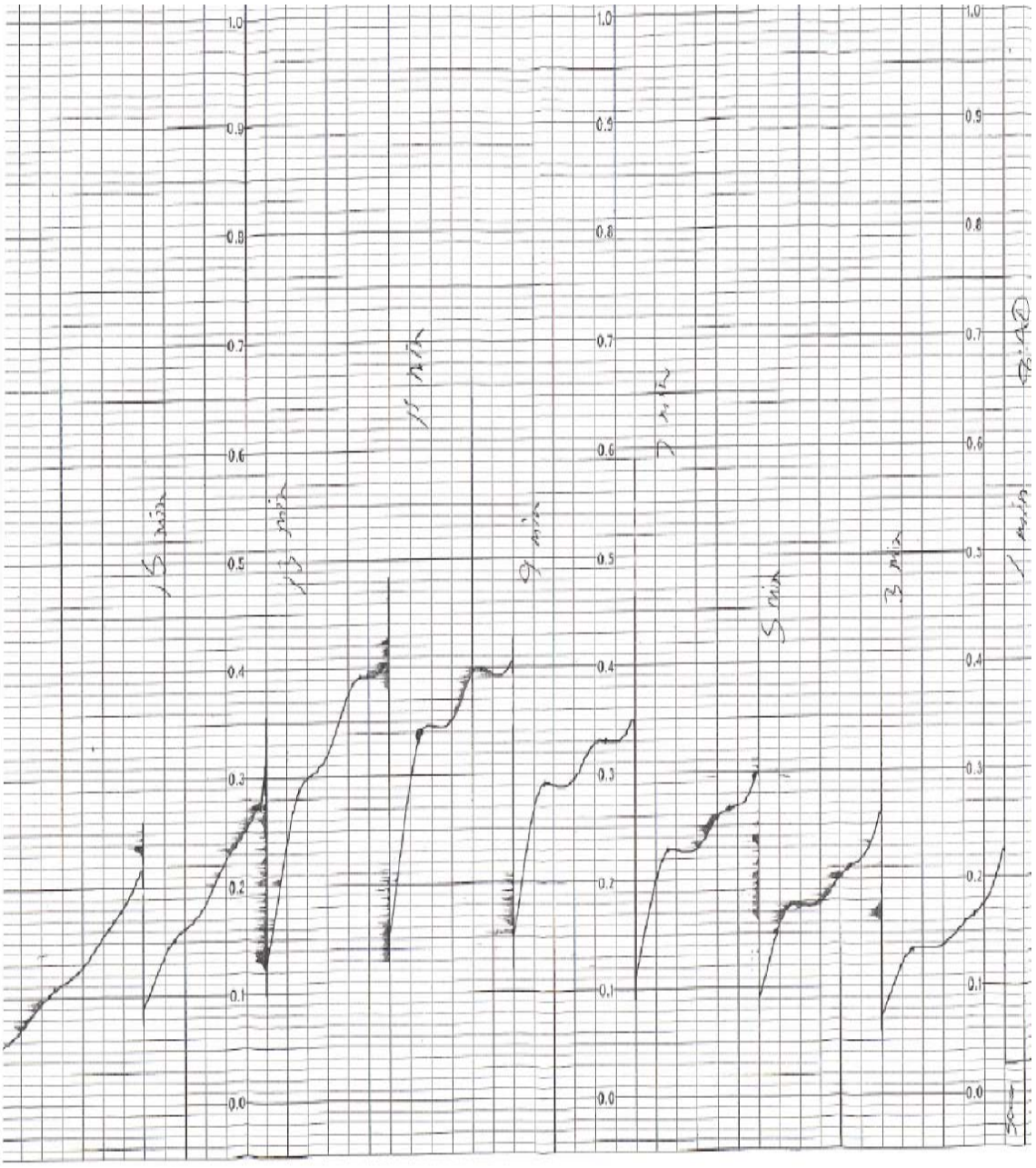

Figure 5: Spectra for Reaction between Cu(II)SalPAHP·2-MeIm and Hydrogen Peroxide Showing the Presence of Two Intermediates*

*Spectra acquired at start times of 1, 3, 5, 7, 9, 11, 13, & 15 minutes. Scans were started at 400 nm and ended at 460 nm. Chart runs from right to left. Test conditions were: 0.0001 M $[CuSalPAHP]_2$; 0.001 M 2-MeIm, and 0.00065 M H_2O_2 (initial).

containing 2-MeIm, the $[CuSalPAHP]_2$ concentration range for the kinetics tests was set as 0.0001 - 0.0003 M in order to capture complete absorbance versus time plots. Appendix B contains the TableCurve data files referenced in this thesis. These printouts show the polynomial data fit including the polynomial equation, the correlation coefficient for the data fit, and the coefficients for the "b" terms, which were used as the value for the estimated initial rate of formation of the first intermediate.

Figure 6 provides a graphical representation of one of the tests run with solutions containing the three different imidazole derivatives. The tabular data for these tests (read from the Cary 14 strip-charts) is given in Appendix 1. It is important to note that the data plots in Figure 6 are composite data points from spectra taken at timed intervals and not continuous absorbance versus time plots. They were useful for demonstrating the relative magnitude of the formation of the copper complex intermediate but were not used to make any conclusions about the timing of when maximum concentrations of intermediates were reached. This is especially relevant in the case of the 2-MeIm solution whereby the peak was off-scale for the reading at 7.5 minutes of elapsed time. However, continuous absorbance versus time plots were used for the kinetics tests.

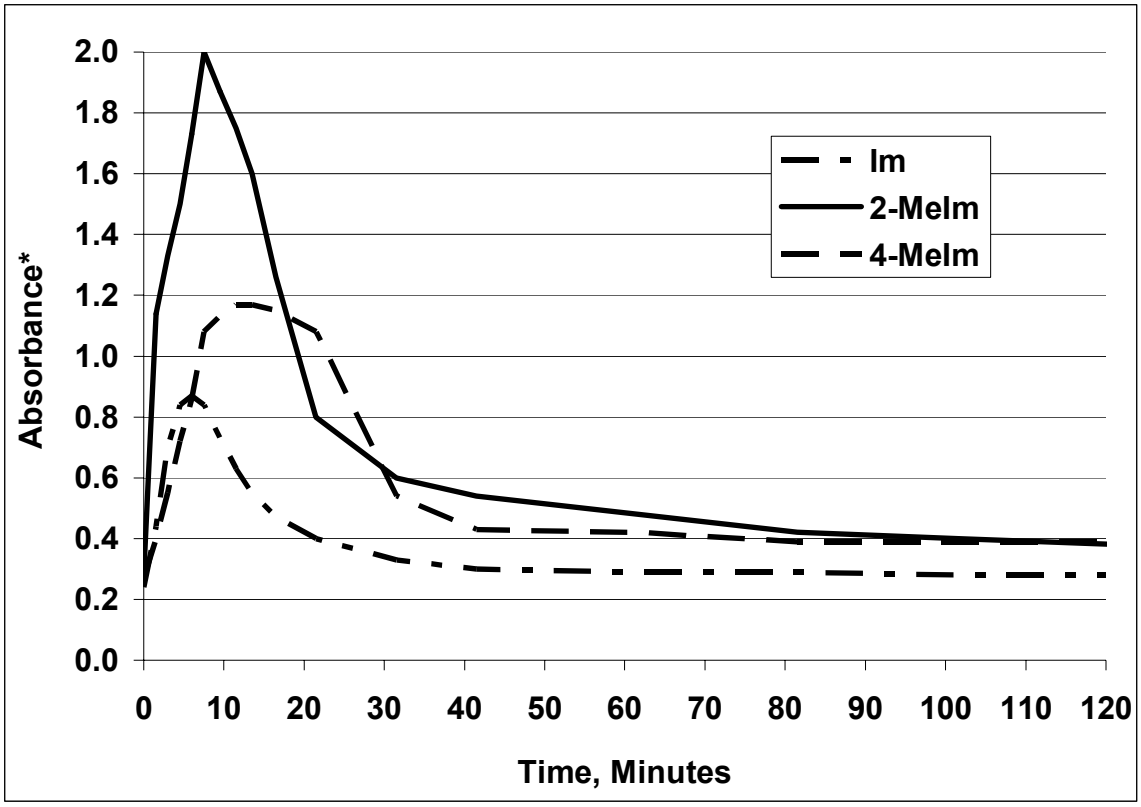

Figure 6: Initial Evaluation of Imidazole Derivatives ([Im Derivative] = 0.01 M; & $[H_2O_2]$ = 0.003 M)

*Im & 4-MeIm intermediate peaks at 448 nm; 2-MeIm intermediate peak at 445 nm.

Kinetics Study

A series of kinetics tests were performed in order to attempt to deduce to the mechanism by which Cu(II)SalPAHP·2-MeIm catalytically decomposes hydrogen peroxide. Initially the initial rate estimation results were very erratic and unpredictable. After a great deal of test protocol troubleshooting and review, the problem with data consistency was tracked back to sample preparation.

It was determined that the order of solvent addition played a role in whether or not a highly reactive "active" complex was created. As was noted above, if water was present during the reaction of the $[CuSalPAHP]_2$ with 2-MeIm, a greenish-blue

intermediate formed that slowly decayed away leaving the typical purplish-blue hue. Spectra obtained from copper complexes exhibiting this formation-induced greenish-blue intermediate that appeared to be identical to spectra having the characteristic peaks at 418 and 445 nm obtained when small dosages of peroxide were added to Cu(II)SalPAHP·2-MeIm solutions. This would seem to imply that peroxide was created. It is not presently clear by what mechanism this could have occurred.

It was also observed that once a sample of Cu(II)SalPAHP·2-MeIm was treated with peroxide, allowed to decay until the yellow intermediate at the peak of the reaction had decayed to a greenish-blue shade, and retreated with peroxide, that rate results similar to those obtained when testing the synthesis-induced greenish-blue samples. In both cases, reaction rates are 4 – 5 times higher for these "active" samples when compared to non-active samples with the same concentrations of 2-MeIm and $[CuSalPAHP]_2$.

It is curious to note that once the purplish-blue Cu(II)SalPAHP·2-MeIm was obtained, adding additional water did not recreate the greenish-blue intermediate. An explanation of what is happening during synthesis of Cu(II)SalPAHP·2-MeIm in the presence of water that would produce this intermediate has not been deduced at this time.

The adjustment in the synthesis protocol allowed for reproducible kinetics tests. The three variables evaluated during testing were: $[CuSalPAHP]_2$, 2-MeIm, and hydrogen peroxide concentrations. Series of tests were performed in which two variables were held constant and one variable was systematically changed. Tables 1, 2, and 3 provide the data from these tests. In addition to the reagent levels and initial rates estimated from TableCurve software, the statistical goodness of fit values (R^2), absorbance (D) at 445 nm

before peroxide addition, absorbance (D) at 445 nm after 30 seconds of elapsed time, and the TableCurve data file number. Appendix 2 contains the printouts for the data files referenced in this thesis.

Table 1: Effect of Varying Initial Hydrogen Peroxide Concentration on Initial Reaction Rate (constant $[CuSalPAHP]_2$ and [2-MeIm])

[Cu(II)], M (10^{-4})	**[2-MeIm], M (10^{-4})**	**[H_2O_2], M (10^{-4})**	**k, s^{-1} (10^{-4})**	**$D_{initial}$**	**$D_{t=30s}$**	**R^2**	**Data File**
2.0	30	5	56	0.08	0.16	0.9998	88
2.0	30	10	93	0.08	0.19	0.9999	87
2.0	30	15	103	0.08	0.22	0.9999	86
2.0	30	20	111	0.08	0.24	0.9999	85
2.0	30	25	121	0.08	0.25	0.9999	82
2.0	30	25	123	0.08	0.125	0.9998	81

Table 2: Effect of Varying 2-Methylimidazole Concentration on Initial Reaction Rate (constant $[CuSalPAHP]_2$ and $[H_2O_2]$)

[Cu(II)], M (10^{-4})	**[2-MeIm], M (10^{-4})**	**[H_2O_2], M (10^{-4})**	**k, s^{-1} (10^{-4})**	**$D_{initial}$**	**$D_{t=30s}$**	**R^2**	**Data File**
2.0	20	25	102	0.08	0.22	0.9999	73
2.0	20	25	97	0.08	0.21	0.9999	79
2.0	30	25	123	0.08	0.25	0.9998	81
2.0	30	25	121	0.08	0.25	0.9999	82
2.0	40	25	98	0.08	0.21	0.9999	75
2.0	40	25	98	0.08	0.22	0.9999	83
2.0	50	25	67	0.08	0.16	0.9999	77
2.0	50	25	56	0.08	0.17	0.9999	78

Table 3: Effect of Varying $[CuSalPAHP]_2$ Concentration on Initial Reaction Rate (constant [2-MeIm] and $[H_2O_2]$)

[Cu(II)], M (10^{-4})	**[2-MeIm], M (10^{-4})**	**[H_2O_2], M (10^{-4})**	**k, s^{-1} (10^{-4})**	**$D_{initial}$**	**$D_{t=30s}$**	**R^2**	**Data File**
1.0	30	25	42	0.05	0.11	0.9999	94
1.0	30	25	37	0.05	0.11	0.9999	95
2.0	30	25	123	0.08	0.25	0.9999	81
2.0	30	25	121	0.08	0.25	0.9999	82
3.0	30	25	317	0.10	0.33	0.9999	96
3.0	30	25	267	0.10	0.31	0.9998	97

Tests were also performed using "active" copper complex samples. Tables 4, 5, and 6 contain the data from these tests. Due to the somewhat subjective nature of the preparation of the active complex, there was a greater degree of variability in data from tests run under identical test conditions. There is an example of this in Table 4 wherein two tests run under identical conditions has estimated initial rates of 0.0283 and 0.0340 sec^{-1}.

Table 4: Active Copper Complex: Effect of Varying Initial Hydrogen Peroxide Concentration on Initial Reaction Rate (constant $[CuSalPAHP]_2$ and [2-MeIm])

[Cu(II)], M (10^{-4})	**[2-MeIm], M (10^{-4})**	**[H_2O_2], M (10^{-4})**	**k, S^{-1} (10^{-4})**	**$D_{initial}$**	**$D_{t=30s}$**	**R^2**	**Data File**
2.0	30	2.9	103	0.08	0.21	0.9999	59
2.0	30	4.0	137	0.08	0.25	0.9993	58
2.0	30	5.0	145	0.08	0.28	0.9999	57
2.0	30	6.6	160	0.08	0.27	0.9998	56
2.0	30	13	220	0.08	0.34	0.9999	55
2.0	30	25	283	0.08	0.42	0.9998	54
2.0	30	25	340	0.08	0.54	0.9999	53

Table 5: Active Copper Complex: Effect of Varying 2-Methylimidazole Concentration on Initial Reaction Rate (constant $[CuSalPAHP]_2$ and $[H_2O_2]$)

[Cu(II)], M (10^{-4})	**[2-MeIm], M (10^{-4})**	**[H_2O_2], M (10^{-4})**	**k, S^{-1} (10^{-4})**	**$D_{initial}$**	**$D_{t=30s}$**	**R^2**	**Data File**
2.0	25	25	270	0.08	0.42	0.9999	60
2.0	30	25	340	0.08	0.42	0.9999	53
2.0	30	25	283	0.08	0.54	0.9998	54
2.0	40	25	256	0.07	0.41	0.9999	28
2.0	50	25	188	0.08	0.31	0.9999	23
2.0	50	25	184	0.07	0.32	0.9999	29

Table 6: Active Copper Complex: Effect of Varying $[CuSalPAHP]_2$ Concentration on Initial Reaction Rate (constant [2-MeIm] and $[H_2O_2]$)

[Cu(II)], M (10^{-4})	**[2-MeIm], M (10^{-4})**	**[H_2O_2], M (10^{-4})**	**k, S^{-1} (10^{-4})**	**$D_{initial}$**	**$D_{t=30s}$**	**R^2**	**Data File**
1.0	30	25	141	0.06	0.28	0.9973	24
1.0	30	25	162	0.06	0.29	0.9999	48
2.0	30	25	283	0.08	0.42	0.9998	54
2.0	30	25	340	0.08	0.54	0.9999	53
3.0	30	25	436	0.10	0.79	0.9998	25

Figures 7, 8, and 9 contain data from similar evaluations of both active and original non-active samples. Similar trends are present in Figures 7 and 8 (varying initial peroxide dosage and varying 2-MeIm concentration). The trends are different in Figure 9 however. The data from the active species is a virtual straight line while the data plot from the non-active samples has upward curvature.

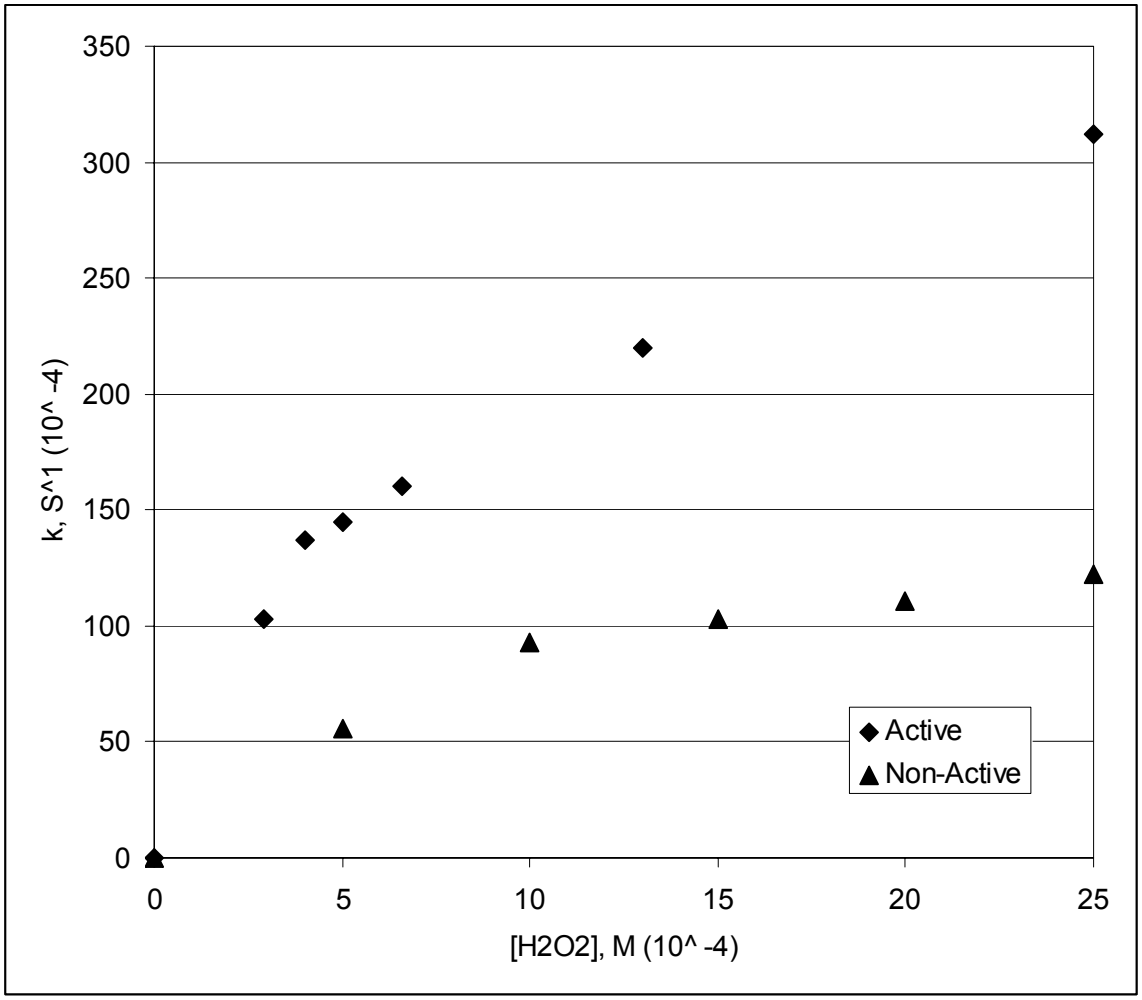

Figure 7: Effect of Varying Initial Hydrogen Peroxide Concentration on Initial Reaction Rate (constant $[CuSalPAHP]_2$ and [2-MeIm])

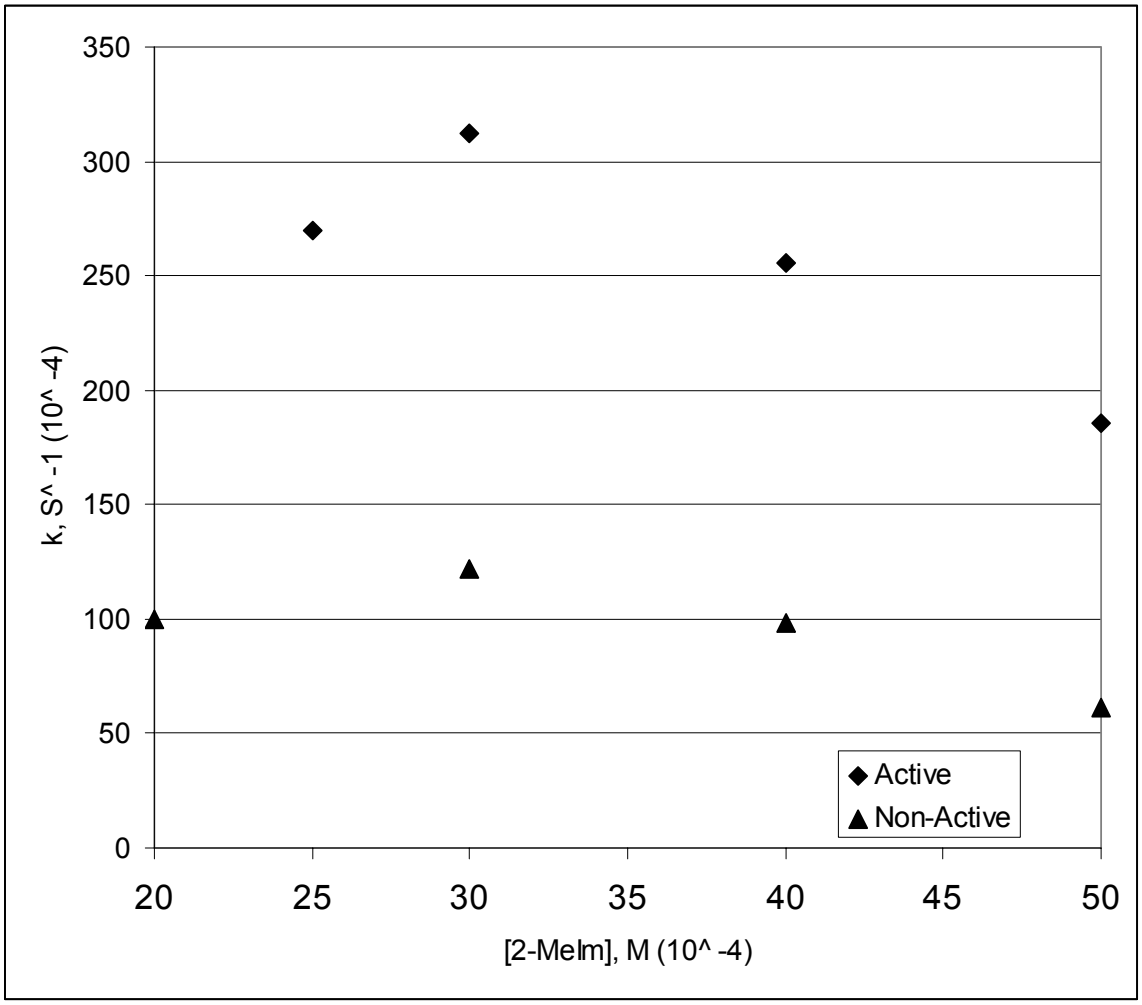

Figure 8: Effect of Varying 2-Methylimidazole Concentration on Initial Reaction Rate (constant $[CuSalPAHP]_2$ and $[H_2O_2]$)

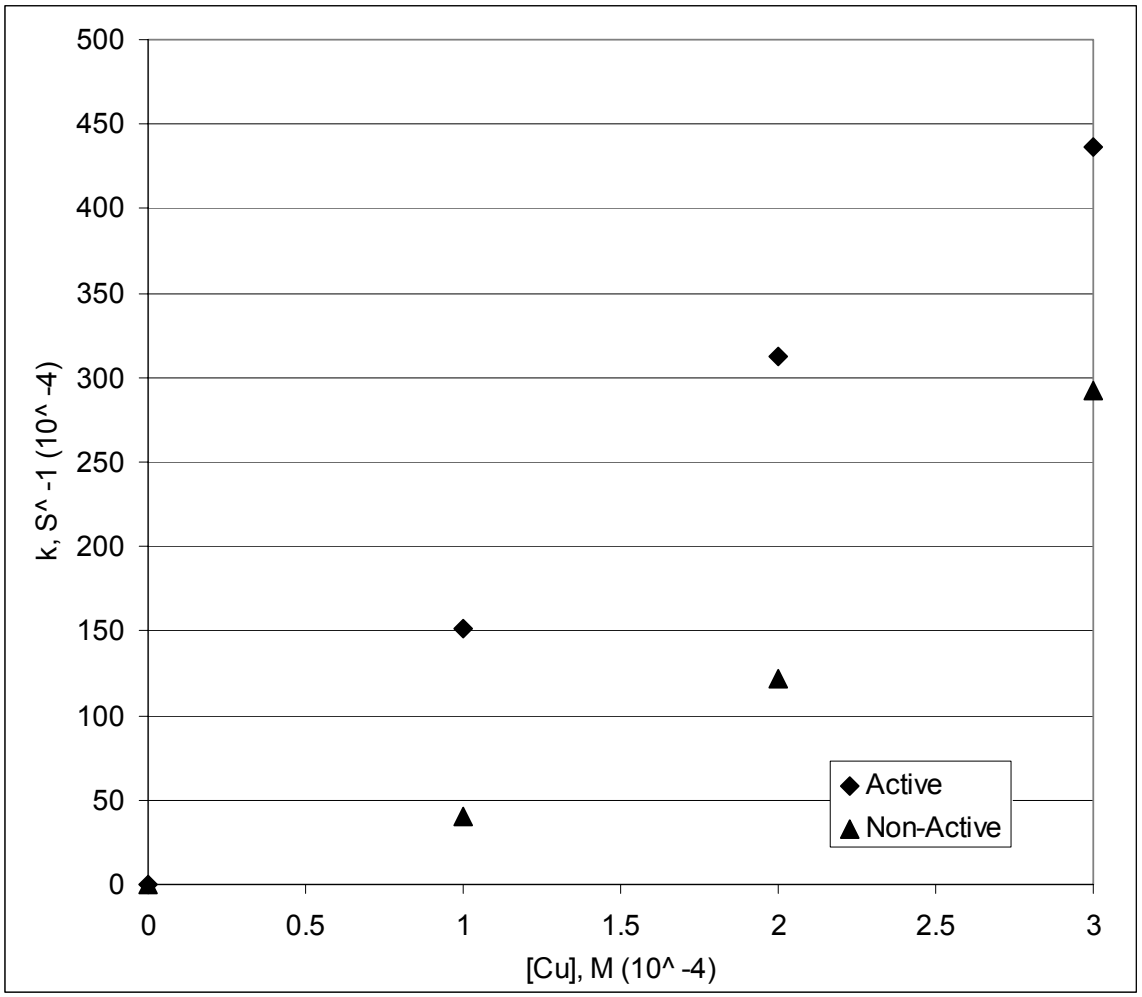

Figure 9: Effect of Varying $[CuSalPAHP]_2$ Concentration on Initial Reaction Rate (constant [2-MeIm] and $[H_2O_2]$)

The final piece of missing information was to attempt to answer the question of whether or not the copper ions in the Cu(II)SalPAHP·2-MeIm complex are reduced from +2 to +1 and then oxidized back to +2 to complete the catalytic cycle. As previously discussed above, two positive indicators of the oxidation state of copper are the presence of a spectral peak that can be assigned as a "d-d" transition due to Cu(II) and the color of solutions containing copper (I) and biquinoline. The Cu(II)SalPAHP·2-MeIm complex shows a distinct peak at 595 nm that has been assigned as a d-d transition. Tests were performed in which time versus absorbance plots were obtained for the peaks at 418, 445, and 595 nm. Figure 10 presents an overlay of these three plots for one of these tests. In these tests, the peak at 595 nm stayed at nearly the same intensity until after both intermediates had decayed mostly away. There was a point in most cases where the intensity of the 595 nm peak would drop about 5 - 10% after ~20 minutes of testing and would then start back upwards towards the original intensity.

In one test, a full spectrum was acquired for the Cu(II)SalPAHP·2-MeIm solution before peroxide addition and again when this drop in intensity at 595 nm occurred. The solvent for this sample was ethanol only. Figure 11 provides these two spectra for comparison. The second spectrum does have a lower peak height at 595 nm, but this appears to be compensated for by broadening of the peak. In any case, there were clearly defined d-d transition peaks in all tests throughout each test run.

Tests were attempted using biquinoline as an indicator for the presence of Cu(I); however, when biquinoline was added to solutions of Cu(II)SalPAHP·2-MeIm, the solution started turning pink before peroxide could be added. These tests were discontinued.

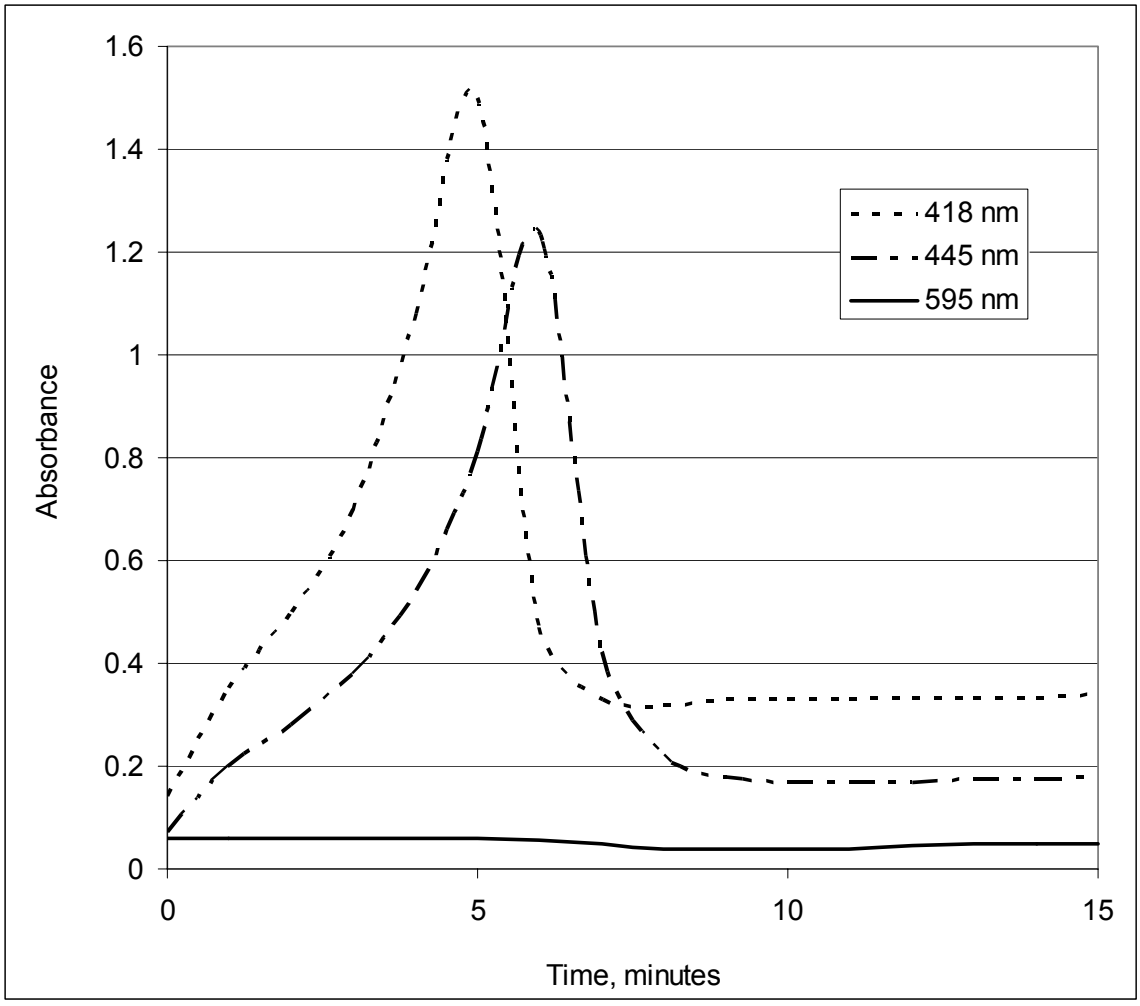

Figure 10: Absorbance Plots at 418, 445, and 595 nm (0.0001 M $[CuSalPAHP]_2$; 0.003 M 2-MeIm; 0.0013 M H_2O_2 (initial))

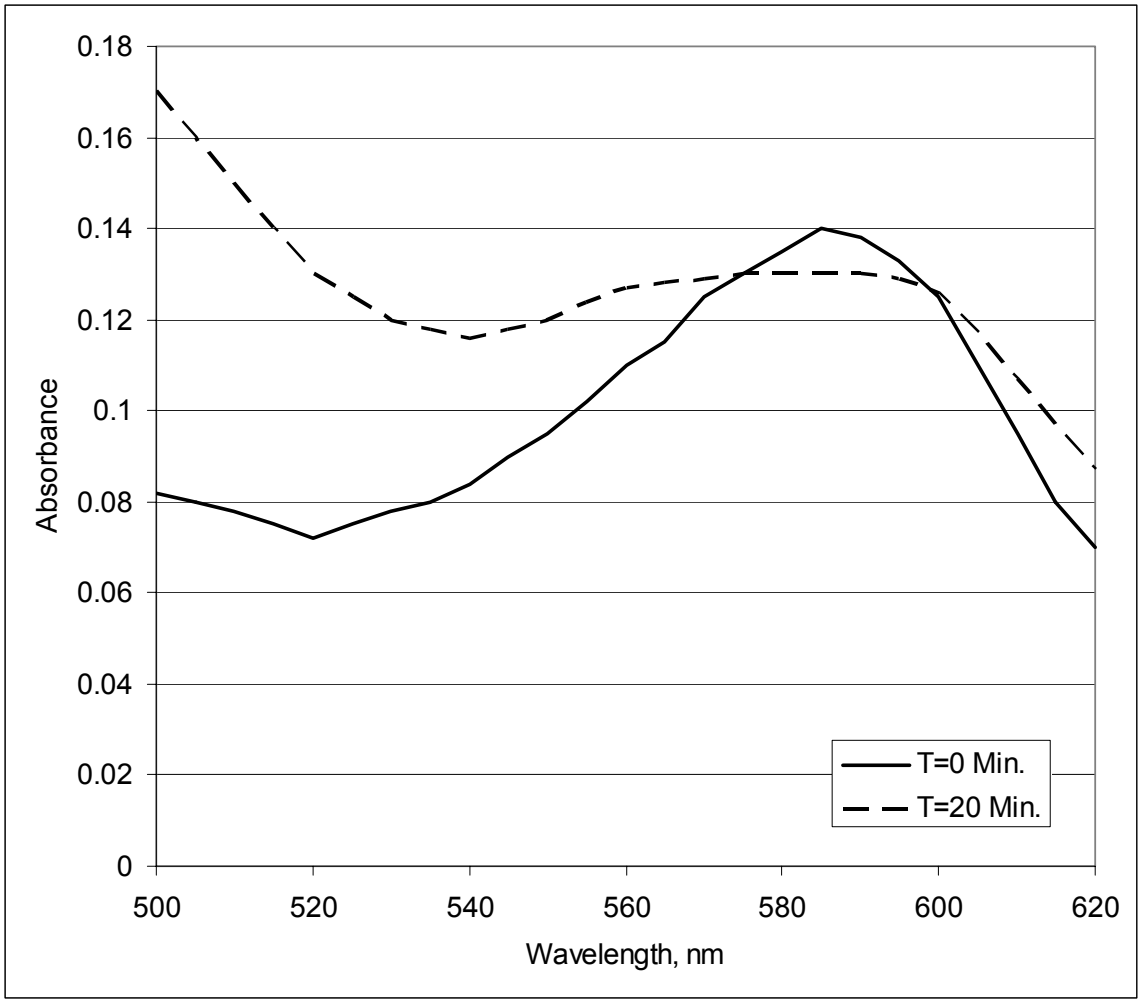

Figure 11: Spectra of Cu(II)SalPAHP·2-MeIm at T=0 and at T=20 Minutes (0.00025 M $[CuSalPAHP]_2$; 0.0075 M 2-MeIm; 0.0013 M H_2O_2 (initial))

CHAPTER 4

DISCUSSION

Preliminary Qualitative Test Results

The initial hypothesis was that affect of changing imidazole substituents would be governed by the different pK_a's of the different derivatives. This hypothesis was based on the belief that hydroxide molecules played a key role in the peroxide decomposition reaction. This trend initially held up as stability to relatively high concentrations of peroxide and spectral intensity of the first intermediate increased in the order of: imidazole, 4-methylimidazole, and 2-methylimidazole. However, 4-nitroimidazole, with the highest pK_a of the imidazole derivatives tested, was unstable. Precipitation of the copper complex was observed almost immediately for samples prepared with 4-NIm. It was not possible to test this complex with peroxide. Another possible role of the imidazole with regards to its affect on CuSalPAHP-Im reactivity is the ability of the imidazole group to stabilize the copper in the Cu(II) oxidation state while it is bound to a peroxide molecule. Previous work with copper(II) diethylenetriamine substituted imidazole complexes identified a property that the researchers called "apparent binding constant, K". This property was described as a quantitative measure of the strength of the Cu-N bond. The Apparent Binding Constants followed the trend: 4-methylimidazole, and 2-methylimidazole. A constant was not measured for 4-nitroimidazole. Table 7 provides pK_a's and pK's (binding) for Im, 4-MeIm, and 2-MeIm. (14) The pK_a for 4-NIm is also included. (15).

Spectral evidence collected during the preliminary qualitative tests point to the existence of two intermediates that have long enough lifetimes to allow for the collection

of spectra. Comparison of the spectra to published spectra and spectral data allow for structures to be assigned to the two intermediates. The first intermediate has been assigned Structure II (Figure 1) based on its intense peak at 445 nm. The second intermediate has been assigned Structure IV based on its intense peak at 418 nm. Although the position of the peak would allow for selection of Structure I, it was not considered because this structure would either require the CuSalPAHP-2-MeIm to be hexa-coordinate or would require that one of the other coordinated Cu-O bonds from the Schiff base to be broken. Structure III was not selected because of the need for an intense peak in the same region as Structure II along with a less intense peak on the higher wavelength shoulder of the primary peak. This peak shape was not observed in this study.

Table 7: Apparent Binding Constants and pK_a's for Imidazole Derivatives

Imidazole Derivative	**pK_a**	**pK**
Imidazole	6.90	0.307
4-Methylimidazole	7.35	-0.084
2-Methylimidazole	7.77	-0.304
4-Nitroimidazole	9.20	NA

Kinetic Tests Results

After reviewing several of the curve-fits, it was apparent that at a point somewhere between 30 and 60 seconds the growth of the peak at 418 nm was significantly affecting the initial rate estimations. To minimize this effect, the initial rate estimations presented in Tables 1 – 6 are based on the first 30 seconds of the reaction after peroxide addition.

The kinetics tests data indicates the existence of both consecutive and competing reactions. The kinetics tests were designed to allow for comparison plots to be prepared. The plot of Cu(II) concentration versus rate (Figure 9) shows that the reaction with regards to copper is first order in the case of the active species but appears to be second order with respect to copper for the non-active species. The plot of initial hydrogen peroxide concentration versus rate (Figure 7) seems to indicate the presence of a maximum level of peroxide dosage that can be handled by a certain concentration of copper complex. Indeed, it was observed that the addition of too much peroxide led to the irreversible precipitation of the copper complex. It is possible that the curve in Figure 7 represents a composite of saturation of the copper complex with peroxide as peroxide dosage was increased and the increased significance of the irreversible precipitation reaction for the tests in which the highest peroxide dosages were used.

The plot of 2-MeIm versus rate (Figure 8) indicates competing reactions. Initially, as the imidazole was increased, reaction rates clearly increased and reached a maximum level. This result was expected because the initial hypothesis for a reaction mechanism involved the need for a hydroxide species in the peroxide decomposition reaction. The downward turn in reaction rate as additional 2-MeIm was added past the

maximum rate point described above was attributed to increasing competition of the excess 2-MeIm for the coordination site on which peroxide bonded. These two reactions would be:

$CuIm + Im \leftrightarrow CuIm_2$ (Equation 4 below)

$CuIm + HO_2^- \rightarrow CuIm(HO_2^-)$ (Equation 5 below)

Based on the results from the both the kinetics tests and the scoping tests, the following mechanism is proposed (Cu = CuSalPAHP moiety; Im is generic imidazole):

Eq. 1: $Im + H_2O \leftrightarrow ImH^+ + OH^-$; K_b

Eq. 2: $H_2O_2 + Im \leftrightarrow HO_2^- + ImH^+$; $K_{a(H2O2)}$

Eq. 3: $Cu_2 + 2\ Im \leftrightarrow 2\ CuIm$; k_1

Eq. 4: $CuIm + Im \leftrightarrow CuIm_2$; k_2 (competitive reaction that impedes HO_2^- bonding with Cu)

Eq. 5: $CuIm + HO_2^- \rightarrow CuIm(HO_2^-)$; k_3 (I1 formed)

Eq. 6: $I1 + HO_2^- \rightarrow CuIm(HO_2)_2^{2-}$; k_4 (T1 formed)

Eq. 7: $I1 + CuIm \rightarrow [(CuIm)_2HO_2^-]$; k_5 (I2 formed)

Eq. 8: $T1 \rightarrow CuIm + 2\ OH^- + O_2$; k_6 (HO_2^- on Cu reduced and second HO_2^- is oxidized)

Eq. 9: $T1 + CuIm \rightarrow (CuIm)_2(HO_2)_2^{2-}$; k_7 (T2 formed)

Eq. 10: $T2 + OH^- \rightarrow I2 + H_2O + O_2$; k_8

Eq. 11: $I2 + HO_2^- \rightarrow 2\ I1$; k_9 (explains higher rate of I1 formation in tests with "activated" CuIm)

Eq. 12: $I2 + OH^- \rightarrow (CuIm)_2O_2 + H_2O$; k_{10} (T3 formed)

Eq. 13: $T3 \rightarrow 2\ CuIm + O_2$; k_{11}

Eq. 14: $Cu + H_2O_2 \rightarrow$ Cu Ppt; k_{12} (predominates when too much peroxide is added)

The terms “T1”, “T2”, and “T3” were used to denote what are believed to be short-lived transition states. Figure 13 provides a visual reaction pathway for this set of reactions. Figures 14, 15, and 16 detail each of the three catalytic cycles that make up the integrated cycle in Figure 13.

This set of reactions provides good explanations for the data and observations made in this study. There is no requirement in the proposed mechanism for the copper to change oxidations states, which allows for the fairly constant peak intensity for the observed d-d transition. The 2nd Intermediate, I2, was assigned as the primary reactive constituent in the “active” species (results in Tables 4, 5, and 6). The active species also probably contains low concentrations of I1. Equation 9 provides the explanation of why the reaction rates forming the 1st Intermediate, I1, are faster than those for the un-activated species. For every mole of peroxide with the I2, two moles of the I1 are immediately formed. The Equation 1 reaction competes with the Equation 2 reaction with respect to the formation of the I1 which explain the dual role of 2-MeIm for providing hydroxide required to initiate the peroxide decomposition reaction and for competing with peroxide molecules for the reactive coordination site on the copper ions.

The reaction in Equation 10 provides the greatest contribution to the formation of I1 due to the coefficient for I1 concentration (two moles of I1 are formed for every mole of I2 present) thus providing an explanation for the observed second order reaction in Cu(II) (increasing Cu(II) concentration would be expected to drive the reaction towards the Equation 10 route). If most of the copper is in the “active” state, I2, then the addition of increasing levels of Cu(II) would have little effect on the rate of the Equation 11 reaction (I2 concentration already is high in this case) and would drive the reaction

towards the Equation 5 route. These scenarios satisfy the observations and results obtained in testing.

In conclusion, a valuable contribution to field of copper chemistry has been made. The use of the Schiff base along with the imidazole derivative provided the desired effect of forcing the added peroxide molecules to add in the less preferred end-on orientation. This provides the research community with a complex that can simulate the chemistry of biological catalases that exhibit end-on peroxy-Cu(II) bonding for study. The use of the Schiff base and stabilizing imidazoles also induced the copper complex to remain in the Cu(II) state thus forcing the copper(II)-peroxide intermediates to decompose primarily through disproportionation reactions with other peroxide molecules and water in the solvent system.

The study of these reactions has led to an interesting and unique mechanism for the catalytic decomposition of hydrogen peroxide and has opened the door to other studies involving this family of complexes such as determining the nature of the nitrogen-copper coordination bond and why the different imidazole derivatives impact the peroxide disproportionation reaction, designing copper catalysts with specific properties, performing low-temperature studies to extend the lifetimes of the intermediates so that the structure of these intermediates can be confirmed, and determining the nature of the reaction in which the imidazole reacts with the CuSalPAHP dimer in the presence of water to form a reactive peroxide-like intermediate.

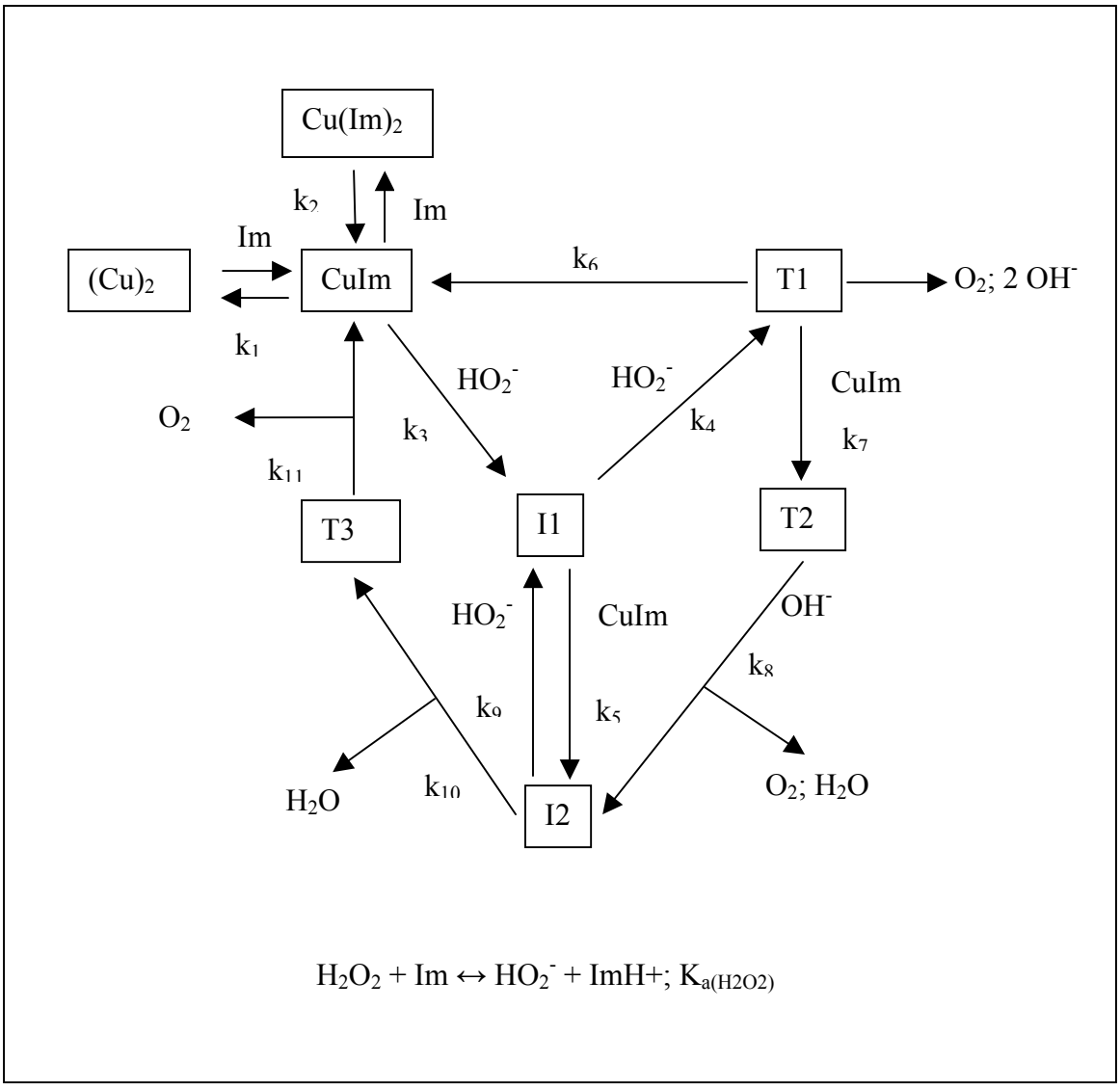

Figure 12: Integrated Catalytic Cycle

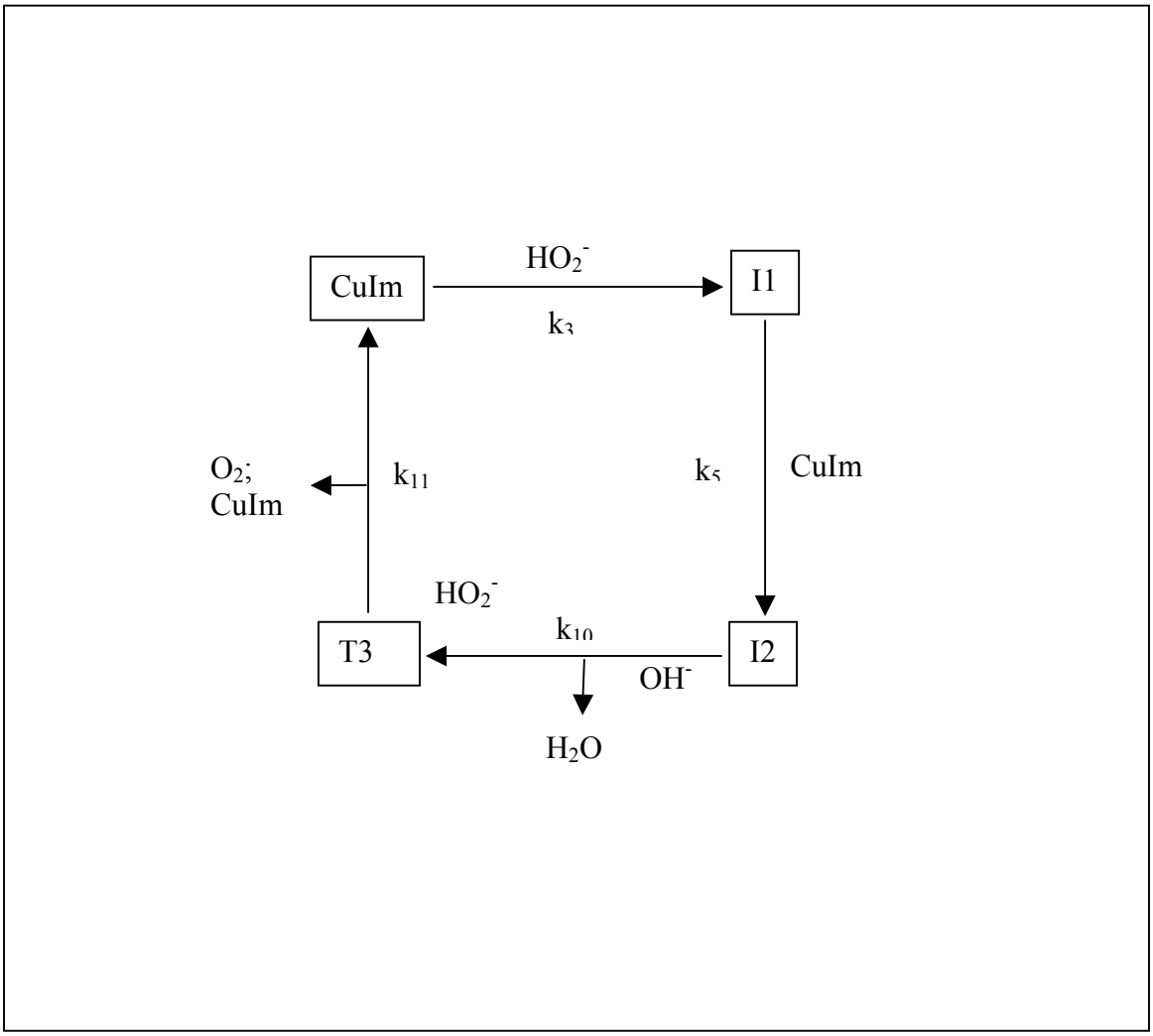

Figure 13: Catalytic Cycle – First Pathway

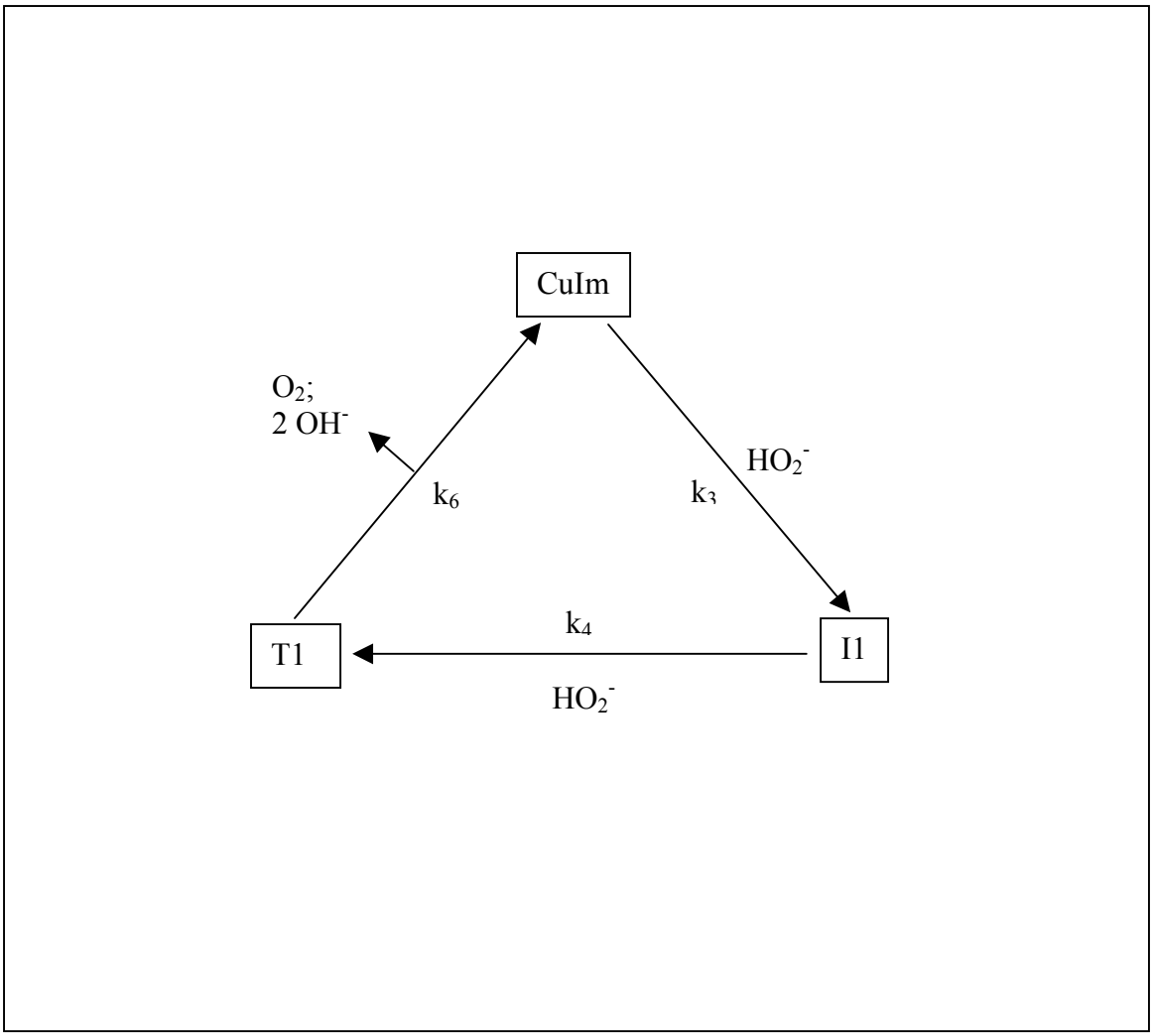

Figure 14: Catalytic Cycle – Second Pathway

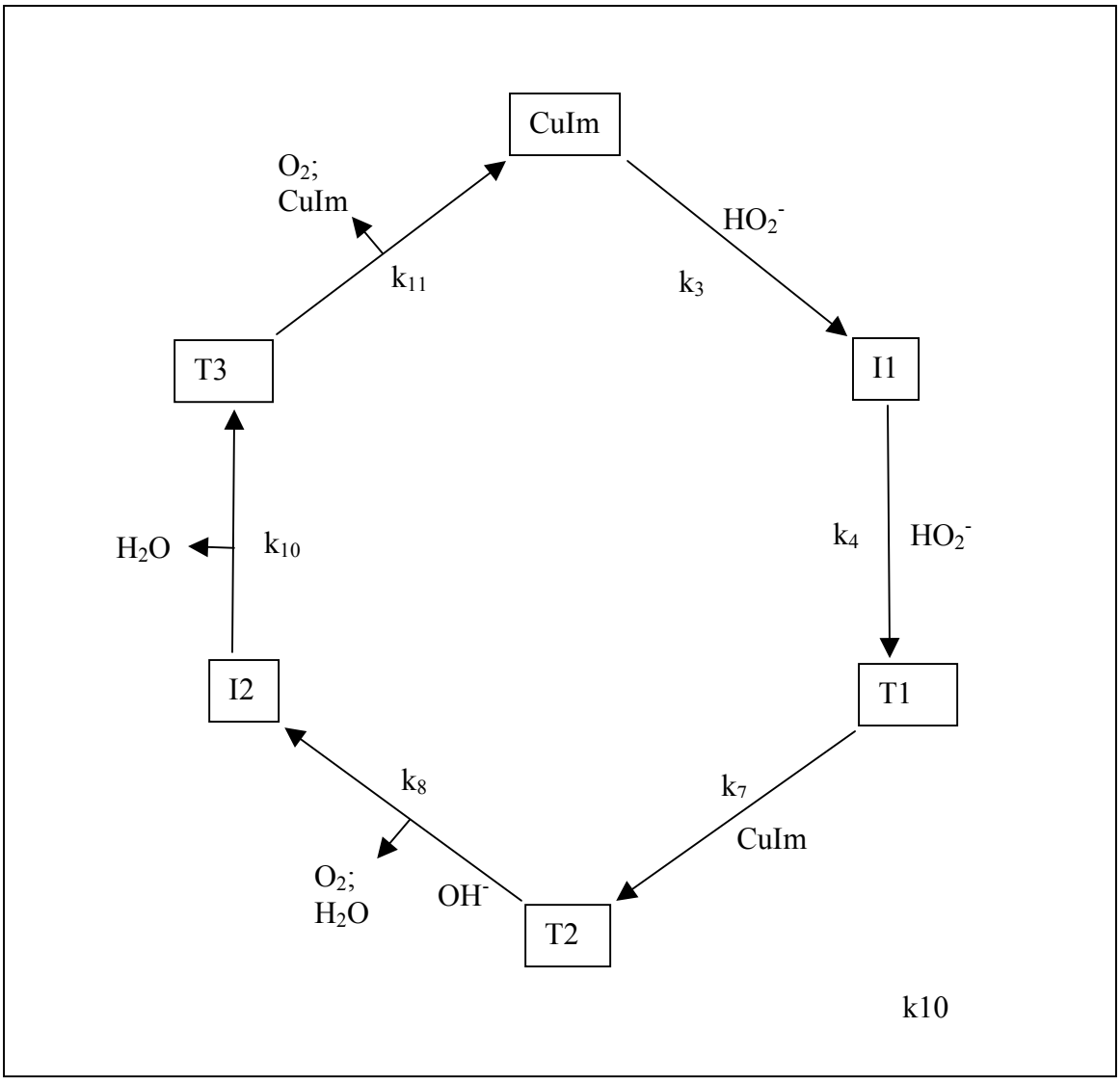

Figure 15: Catalytic Cycle – Third Pathway

REFERENCES

1. Brown, J. C. and Wardeska, J. G., *Characterization of a Dimeric Copper (II) Complex of a Dissymmectric Schiff Base and Its Ligand Adducts*, *Inog. Chem.,* **1982**, *21*, 1530 – 1534.
2. Mahapatra, S., Halfen, J. A., Wilkinson, E. C., Pan, G., Cramer, L. Q. Jr., and Tolman, W. B., *A New Intermediate in Copper Dioxygen Chemistry: Breaking the O-O Bond to Form a {$Cu_2(u\text{-}O)_2$} Core*, *J. Am. Chem. Soc.,* **1995**, *117*, 8865 – 8866.
3. Ross, P. K. and Solomon, E. I., *An Electronic Structural Comparison of Copper-Peroxide Complexes of Relevance to Hemocyanin and Tyrosinase Active Sites*, *J. Am. Chem. Soc.,* **1991**, *113*, 3246 – 3259.
4. Shin, W., Sundaram, U. M., Cole, J. L., Zhang, H. H., Hedman, B., Hodgson, K. O., and Solomon, E. I., *Chemical and Spectroscopic Definition of the Peroxide-Level Intermediate in the Multicopper Oxidases: Relevance to the Catalytic Mechanism of Dioxygen Reduction to Water, J. Am. Chem. Soc.,* **1996**, *118*, 3202 – 3215.
5. Berreau, L. M., Marapatra, S., Halfen, J. A., Young, V. G. Jr., and Tolmon, W. B., *Independent Synthesis and Structural Characterization of a Mononuclear Copper-Hydroxide Previously Assigned as a Copper Superoxide Species, Inorg. Chem.*, **1996**, *35*, 6339 – 6342.

6. Sanyal, I., Mahroof-Tahir, M., Nasir, M. S., Ghosh, P., Cohen, Y. G., Cruse, R. W., Farooq, A., Karlin, K. D., Liu, S., and Zubieta, J., *Reactions of Dioxygen (O_2) with Mononuclear Copper (I) Complexes: Temperature-Dependent Formation of Peroxo- or Oxo- (and Dihydroxo-) Bridged Dicopper Complexes*, *Inorg. Chem.*, **1992**, *31*, 4322 - 4332.

7. Jiang, F., Karlin, K. D., and Peisach, J., *An Electron Spin Echo Envelope Modulation (ESEEM) Study of Electron-Nuclear Hyperfine Nuclear Quadupole Interactions of d_{x^2} Ground State Copper (II) Complexes with Substituted Imidazoles*, *Inorg. Chem.*, **1993**, *32*, 2576 - 2582.

8. Schubert, J. and Sharma, V. S., *Catalytic Activity of Metal Chelates and Mixed-Ligand Complexes in the Neutral pH region. I. Copper-Imidazole*, *J. Am. Chem. Soc.*, **1969**, *91*, 8291 - 8296.

9. Aboella, N. W., Lewis, E. A., Reynolds, A. M., Brennessel, W. W., Cramer, C. J., and Tolman, W. B., *Snapshots of Dioxygen Activation by Copper: The Structure of a 1:1 Cu/O_2 Adduct and Its Use in Synthesis of Asymmetric Bis(u-oxo) Complexes, J. Am. Chem. Soc.*, **2002**, *124*, 10660 - 10661.

10. Hegg, E. L., Mortimore, S. H., Cheung, C. L., Huyett, J. E., Powell, D. R., and Burstyn, J. N., *Inorg. Chem.,* **1999**, *38*, 2961 - 2968.

11. Fawcett, T. G., Bernarducci, E. E., Krogh-Jesperersen, K., and Schugar, H. J., *Charge-Transfer Absorptions of Cu (II)- Imidazole and Cu (II) – Imidazolate Chromophores*, *J. Am. Chem. Soc.,* **1980**, *102*, 2598 - 2604.

12. Chaudhuri, P., Karpenstein, I., Winter, M., Lengen, M., Butzlaff, C., Bill, Eckhard, Trautwein, A. X., Florke, U., and Haupt, H., *An Imiazolate-Bridged Tetranuclear Copper (II) Complex: Synthesis, Magnetic and EPR Studies, and Crystal Structure of* $[L_4Cu_4(Im)_4](ClO_4)_4 . 2 H_2O$ *(L = 1,4,7 – Triazacyclononane Imidazolate Anion)*, *Inorg. Chem*., **1993**, *32*, 888 - 894.

13. Wilkins, R. G., *Kinetics and Mechanisms of Reactions of Transition Metal Complexes*, 2nd Edition, **1991**, 4.

14. Jiang, F., McCracken, J., and Peisach, J., *Nuclear Quadrupole Interactions in Copper(II)-Diethylenetriamine-Substituted Imidazole Complexes and in Copper(II) Proteins, . Am. Chem. Soc.*, **1990**, *112*, 9035 – 9044.

15. Eaton, D. R. and Watkins, J. M., *Chemistry of the Pentacyano(4-Nitroimidazolato)ferrate(II) Ion: Unusual oxidation States of* Iron", *Inorg. Chem*., **1985**, *24*, 1424 - 1431.

APPENDICES

Appendix A: Tabular Absorbance Versus Time Date for Initial Evaluation of Imidazole Derivatives (with $[CuSalPAHP]_2 = 0.001$ M; [Im Derivative] = 0.01 M; & [H2O2] = 0.003 M)

Time, Minutes	**Im Abs.* (Peak @ 448 nm)**	**2-MeIm Abs.* (Peak @ 445 nm)**	**4-MeIm Abs.* (Peak @ 448 nm)**
0	0.24	0.28	0.27
1.5	0.44	1.14	0.40
3.0	0.70	1.33	0.55
4.5	0.84	1.5	0.72
6.0	0.87	1.73	0.86
7.5	0.84	>2.00	1.08
9.5	0.73	1.87	1.13
11.5	0.63	1.75	1.17
13.5	0.55	1.60	1.17
16.5	0.47	1.26	1.15
21.5	0.40	0.80	1.08
31.5	0.33	0.60	0.54
41.5	0.30	0.54	0.43
61.5	0.29	0.48	0.42
81.5	0.29	0.42	0.39
101.5	0.28	0.40	0.39
121.5	0.28	0.38	0.39

* The Cary 14 utilizes a strip-chart recorder with strip-chart paper marked off for absorbance from 0.0 to 1.0. Since the instrument can read in two ranges, the low range readings were taken from the charts with values of 0.0 – 1.0, and the high range readings were taken from the charts with values of 1.0 – 2.0.

Appendix B: TableCurve Data Files

The following printouts are unaltered TableCurve scans of data plots from the data entered from the Cary 14 spectrometer stripcharts. The Test Numbers on each printout correspond to the identification numbers in Tables 1 – 6 in the text.

Appendix B: TableCurve Data Files (con't)

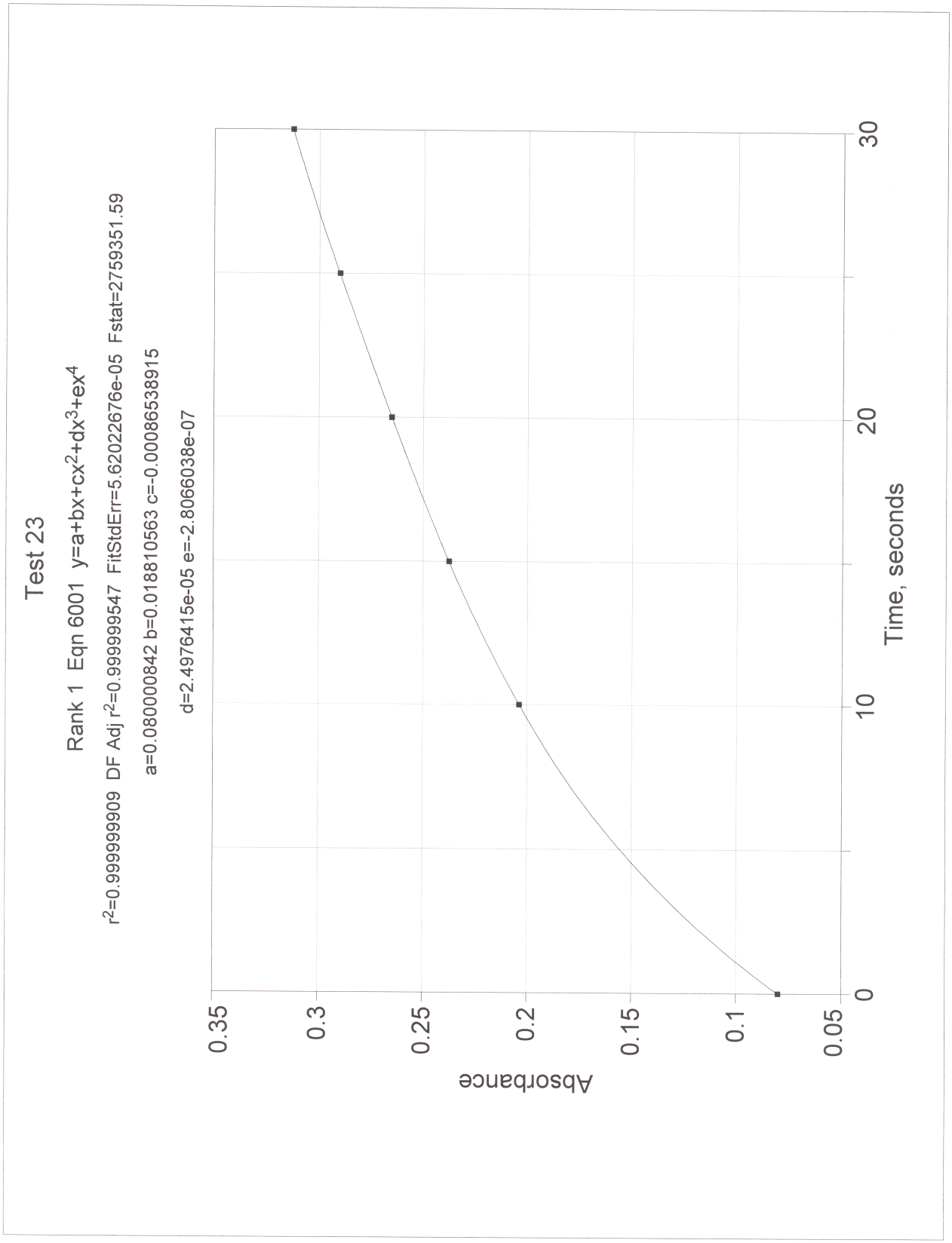

Appendix B: TableCurve Data Files (con't)

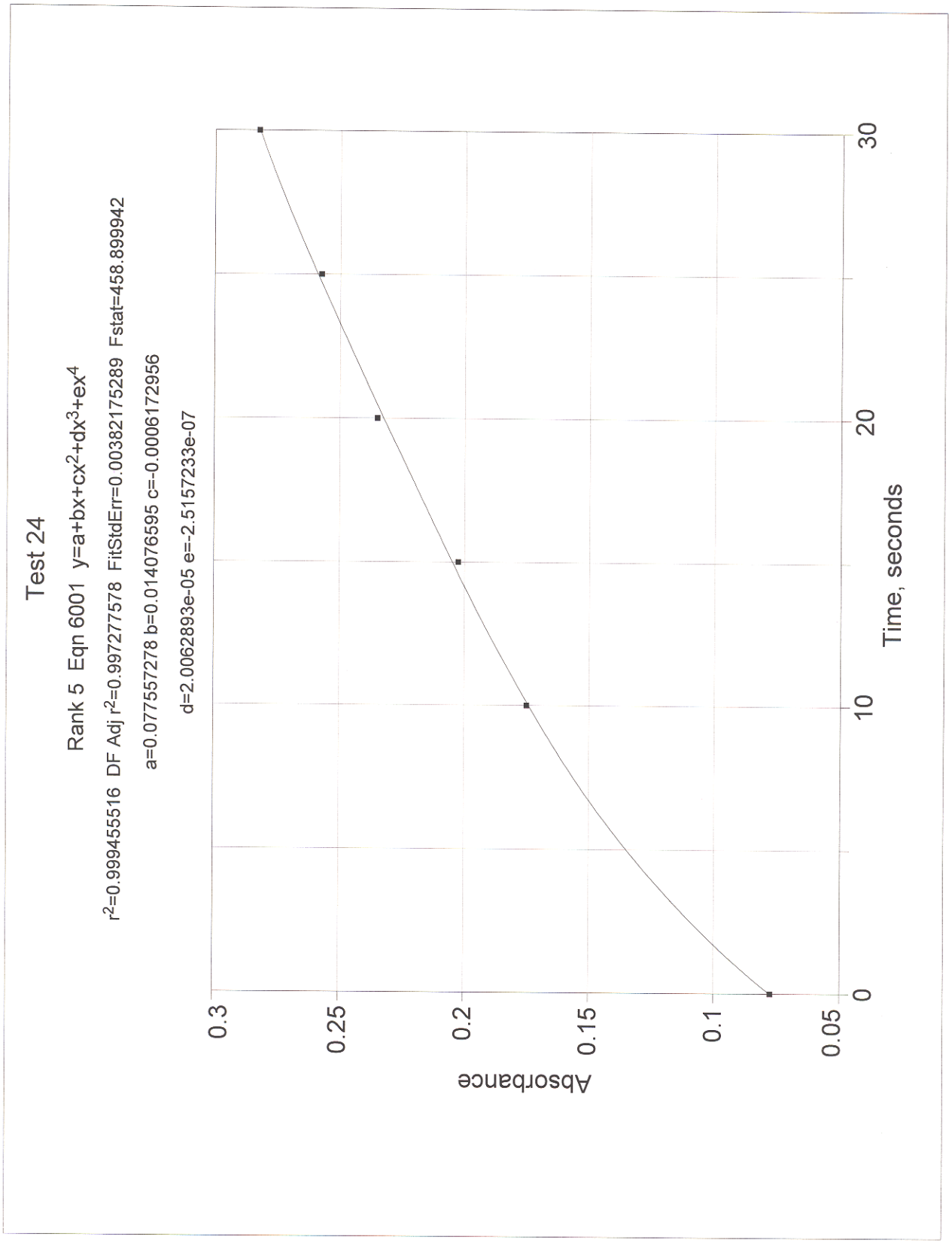

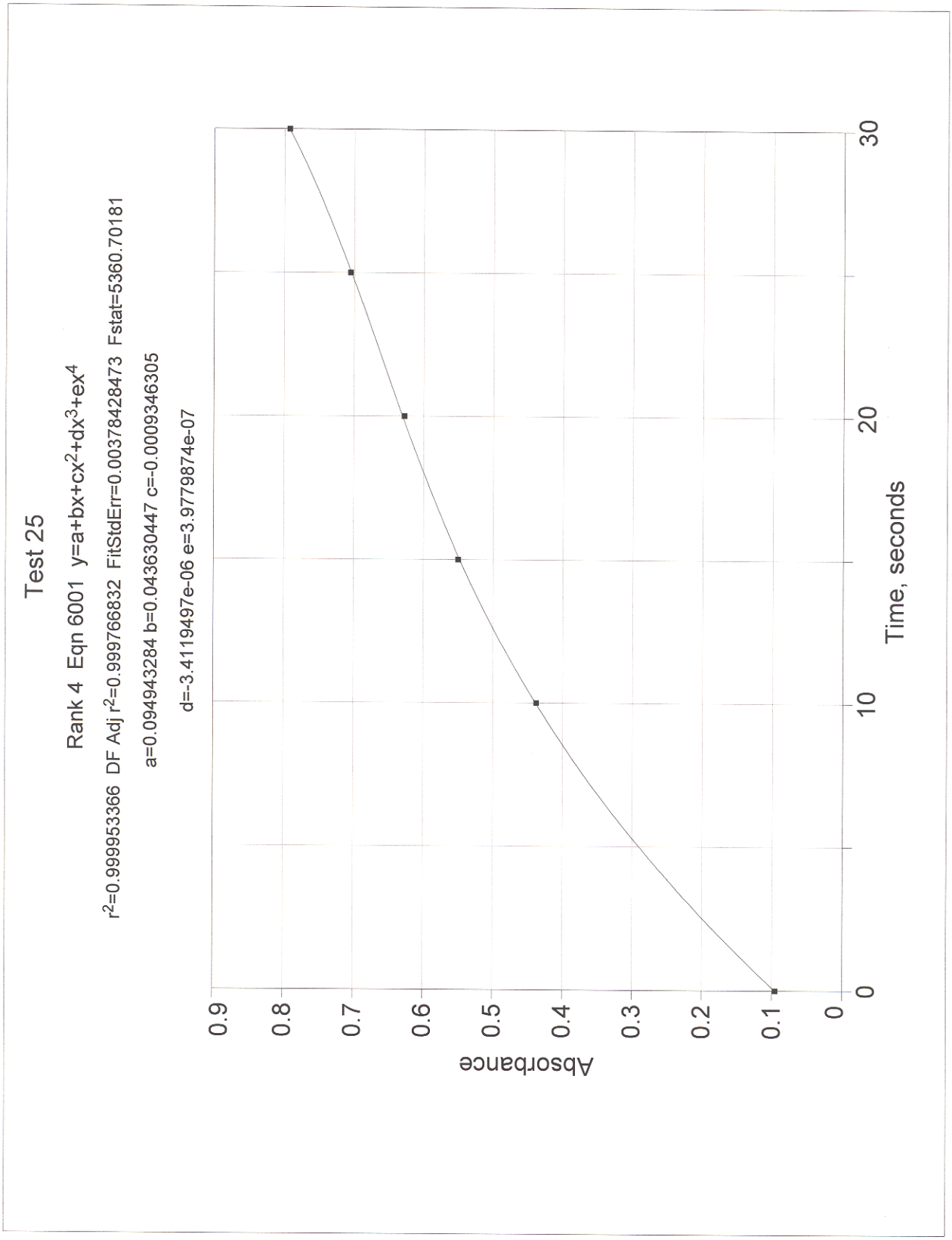
Test 25
Rank 4 Eqn 6001 y=a+bx+cx²+dx³+ex⁴
r²=0.999953366 DF Adj r²=0.999766832 FitStdErr=0.00378428473 Fstat=5360.70181
a=0.094943284 b=0.043630447 c=-0.0009346305
d=-3.4119497e-06 e=3.9779874e-07
Absorbance
0
0.1
0.2
0.3
0.4
0.5
0.6
0.7
0.8
0.9
Time, seconds
0
10
20
30

Appendix B: TableCurve Data Files (con't)

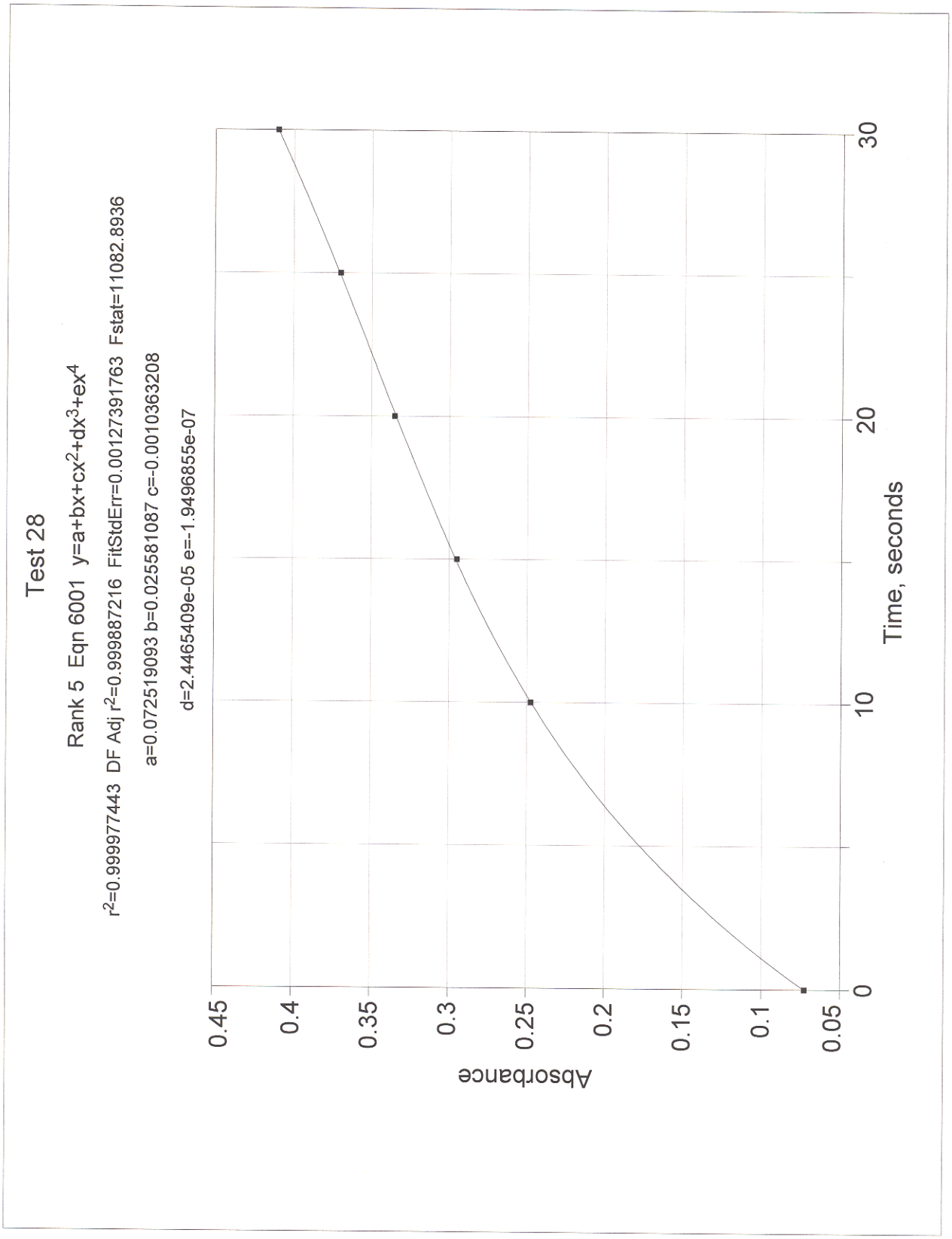

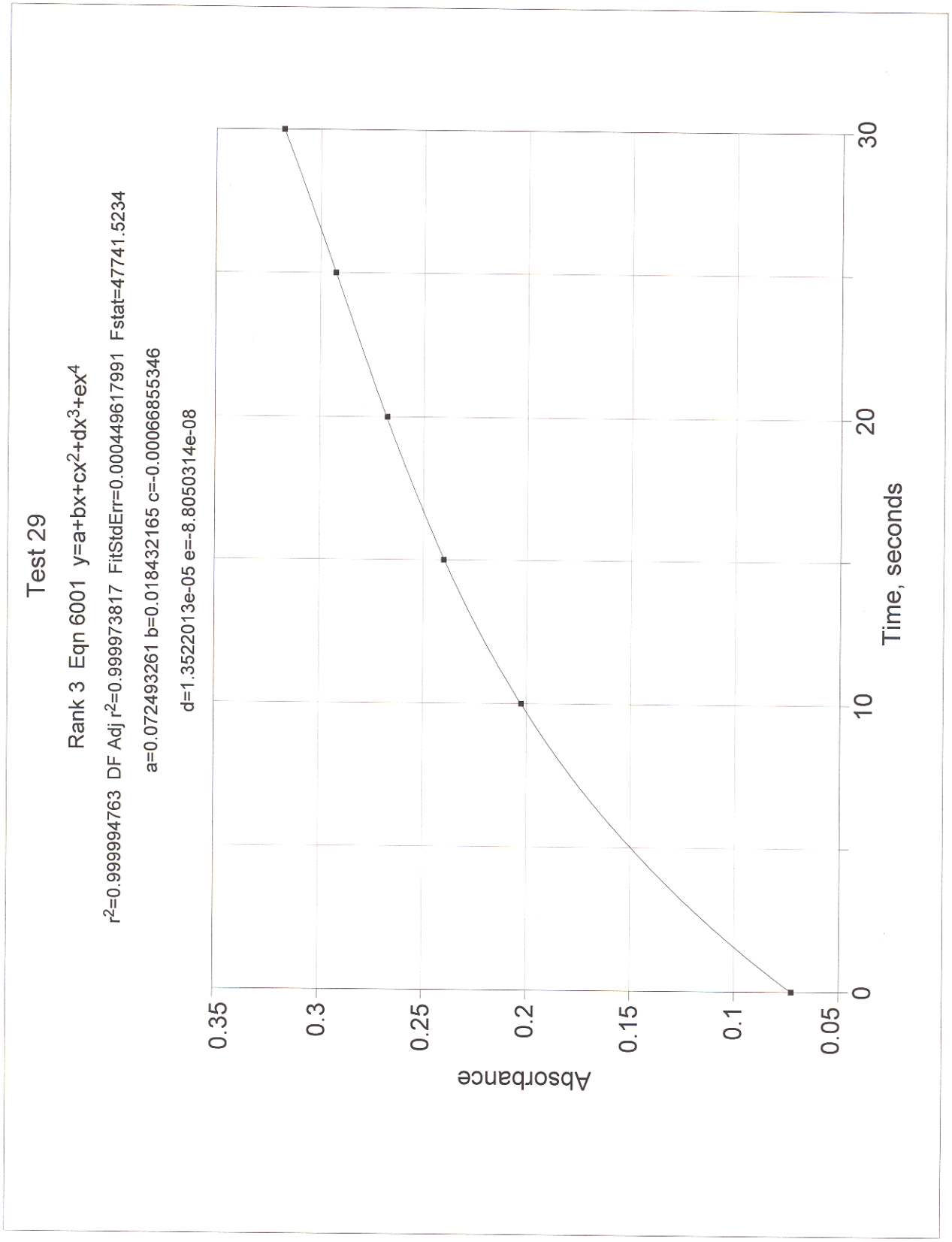
Test 29
Rank 3 Eqn 6001 y=a+bx+cx²+dx³+ex⁴
r²=0.999994763 DF Adj r²=0.999973817 FitStdErr=0.000449617991 Fstat=47741.5234
a=0.072493261 b=0.018432165 c=-0.00066855346
d=1.3522013e-05 e=-8.8050314e-08
Absorbance
0.35
0.3
0.25
0.2
0.15
0.1
0.05
0
10
20
30
Time, seconds

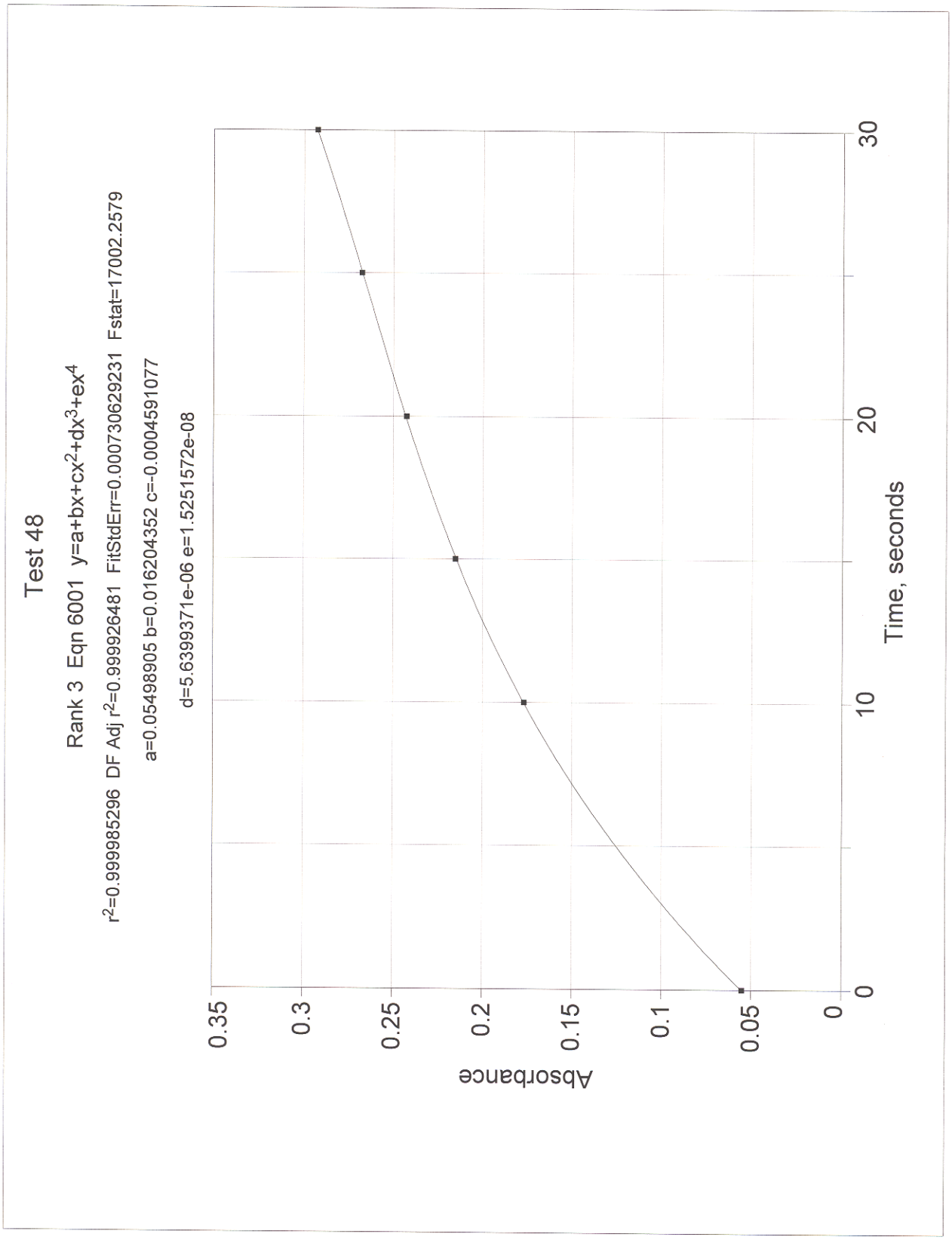
Test 48
Rank 3 Eqn 6001 y=a+bx+cx²+dx³+ex⁴
r²=0.999985296 DF Adj r²=0.999926481 FitStdErr=0.000730629231 Fstat=17002.2579
a=0.05498905 b=0.016204352 c=-0.0004591077
d=5.63993771e-06 e=1.5251572e-08
Absorbance
0.35
0.3
0.25
0.2
0.15
0.1
0.05
0
0
10
20
30
Time, seconds

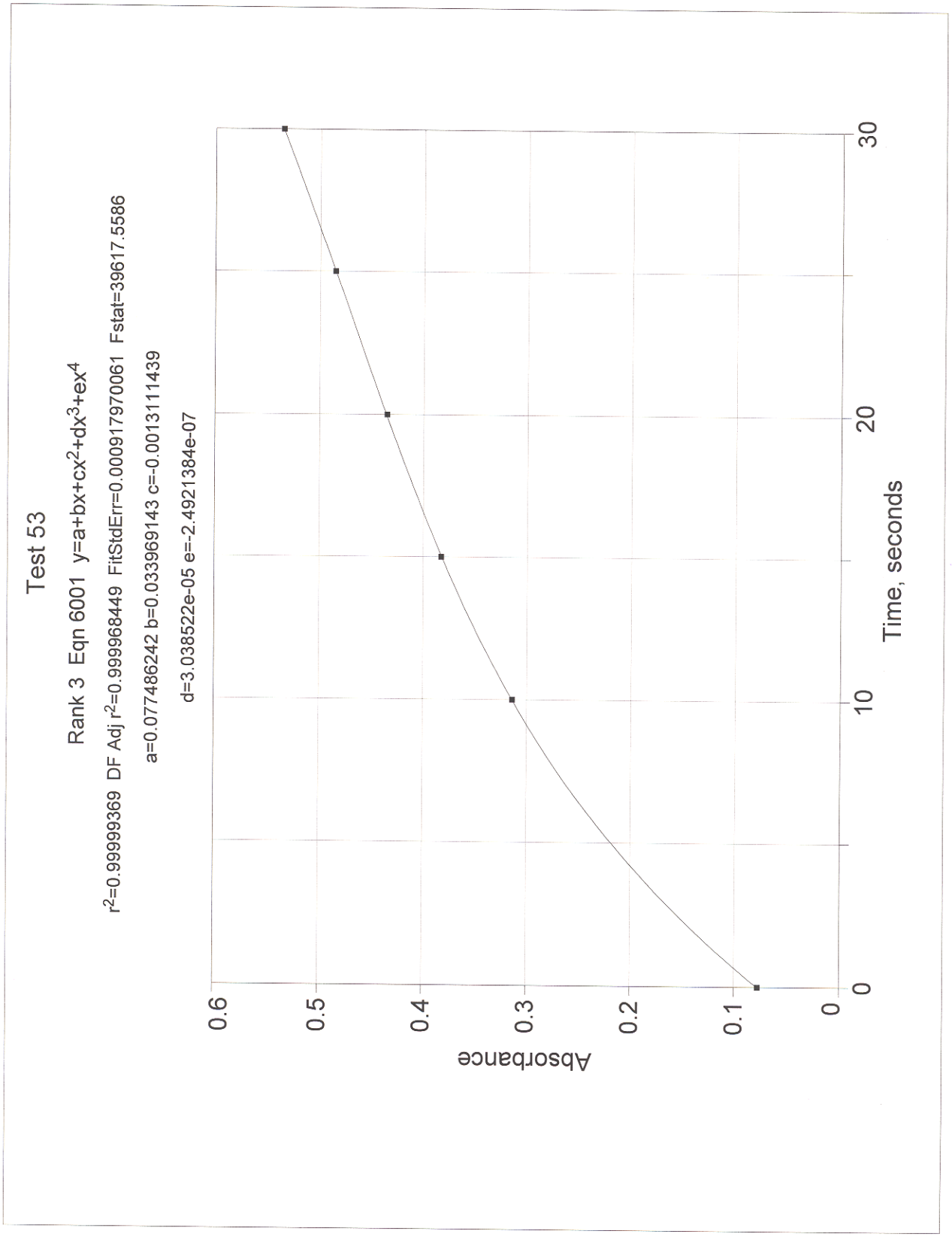
Test 53
Rank 3 Eqn 6001 y=a+bx+cx²+dx³+ex⁴
r²=0.99999369 DF Adj r²=0.999968449 FitStdErr=0.000917970061 Fstat=39617.5586
a=0.077486242 b=0.033969143 c=-0.0013111439
d=3.038522e-05 e=-2.4921384e-07
Absorbance
0
0.1
0.2
0.3
0.4
0.5
0.6
0
10
20
30
Time, seconds

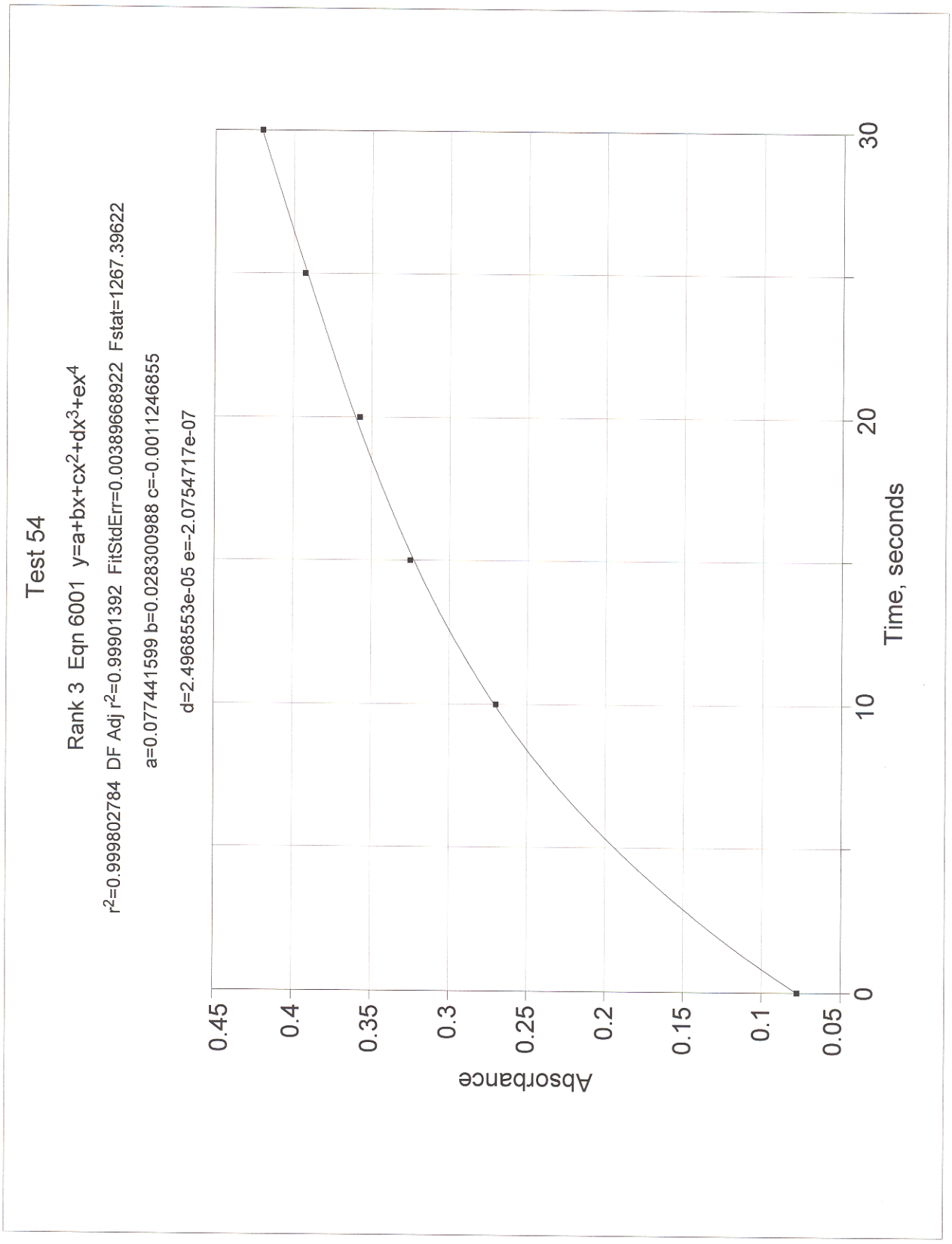
Test 54
Rank 3 Eqn 6001 y=a+bx+cx²+dx³+ex⁴
r²=0.999802784 DF Adj r²=0.99901392 FitStdErr=0.00389668922 Fstat=1267.39622
a=0.077441599 b=0.028300988 c=-0.0011246855
d=2.4968553e-05 e=-2.0754717e-07
Absorbance
0.45
0.4
0.35
0.3
0.25
0.2
0.15
0.1
0.05
0
10
20
30
Time, seconds

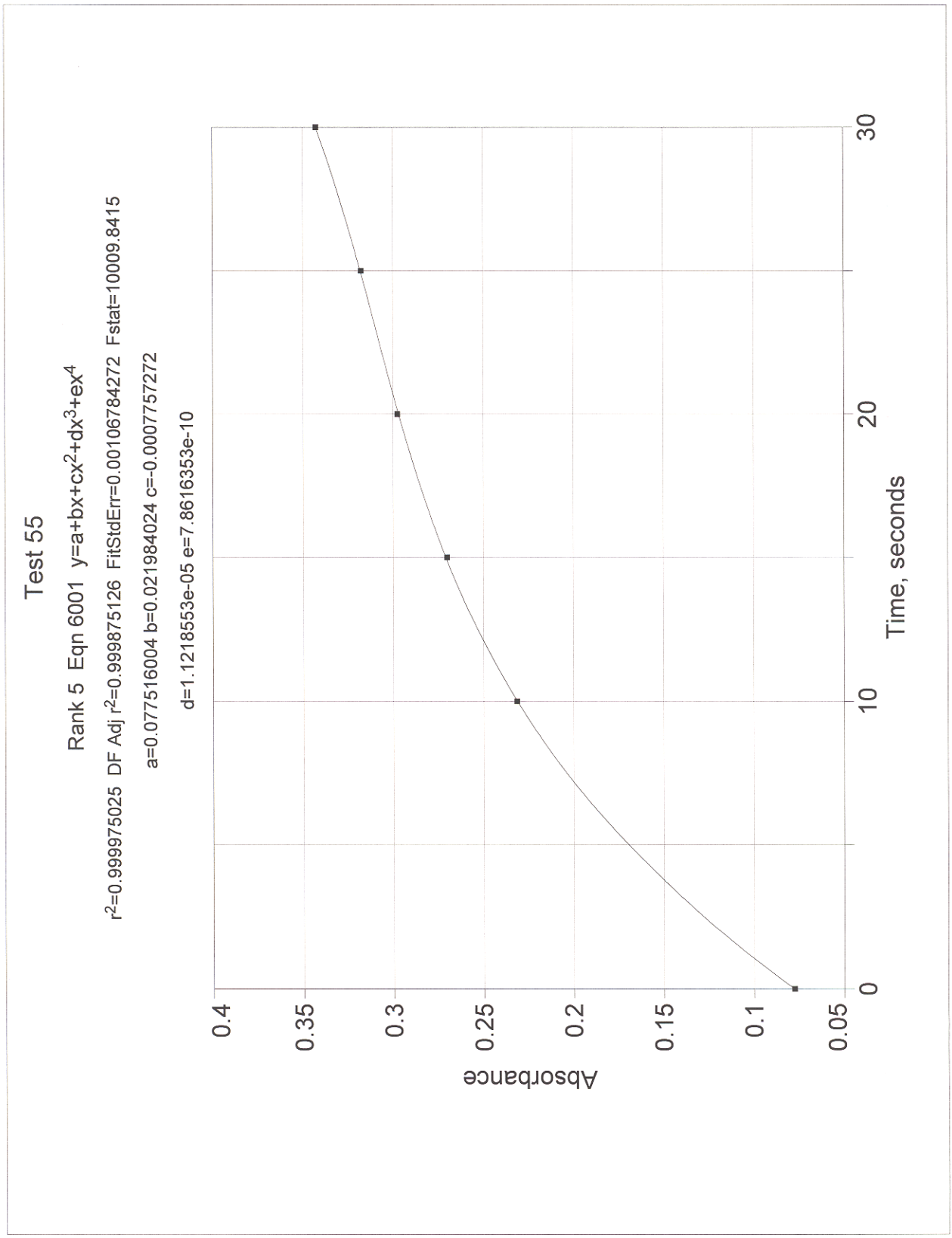
Test 55
Rank 5 Eqn 6001 y=a+bx+cx²+dx³+ex⁴
r²=0.999975025 DF Adj r²=0.999875126 FitStdErr=0.00106784272 Fstat=10009.8415
a=0.077516004 b=0.021984024 c=-0.0007757272
d=1.1218553e-05 e=7.8616353e-10
Absorbance
0.4
0.35
0.3
0.25
0.2
0.15
0.1
0.05
0
10
20
30
Time, seconds

Appendix B: TableCurve Data Files (con't)

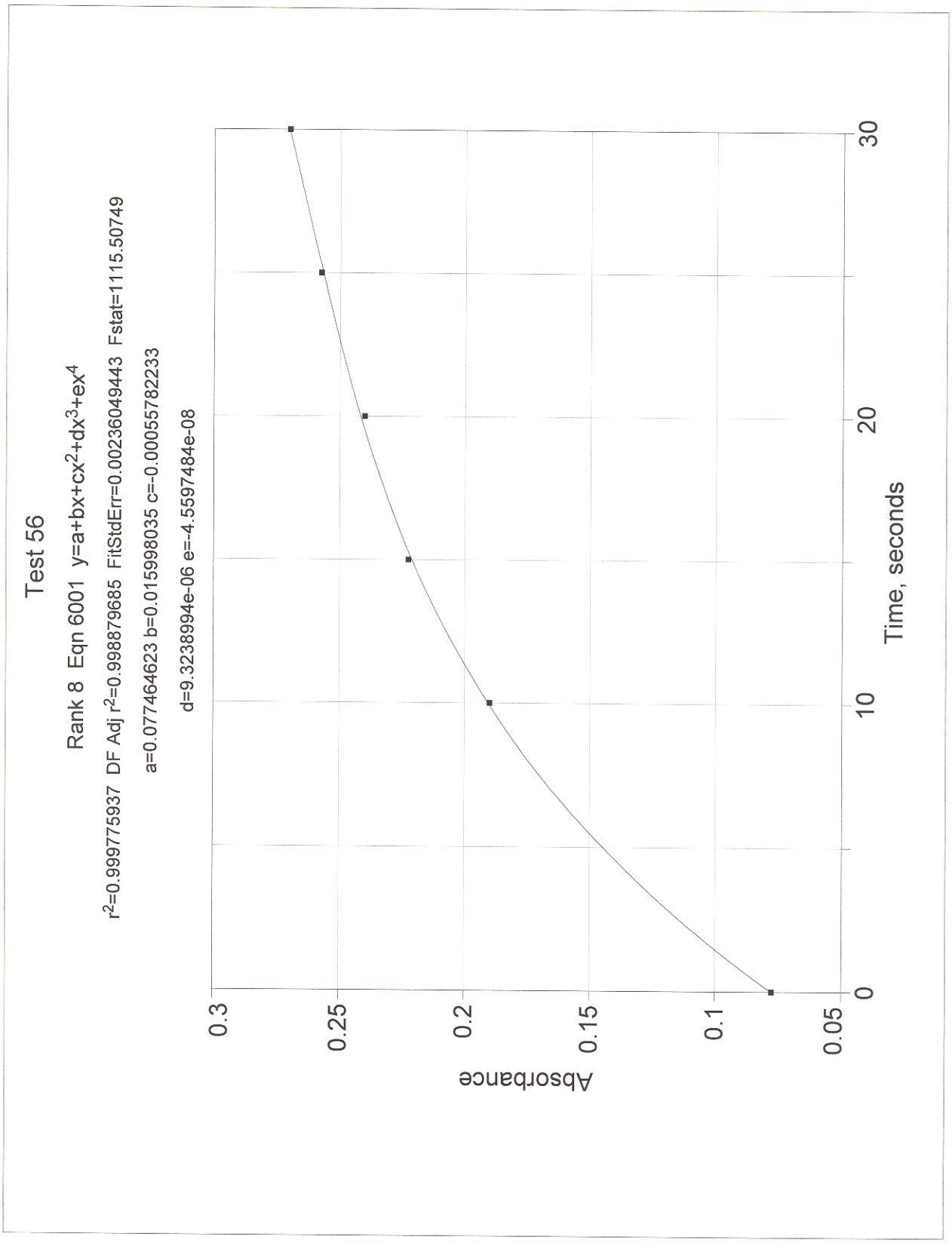

Appendix B: TableCurve Data Files (con't)

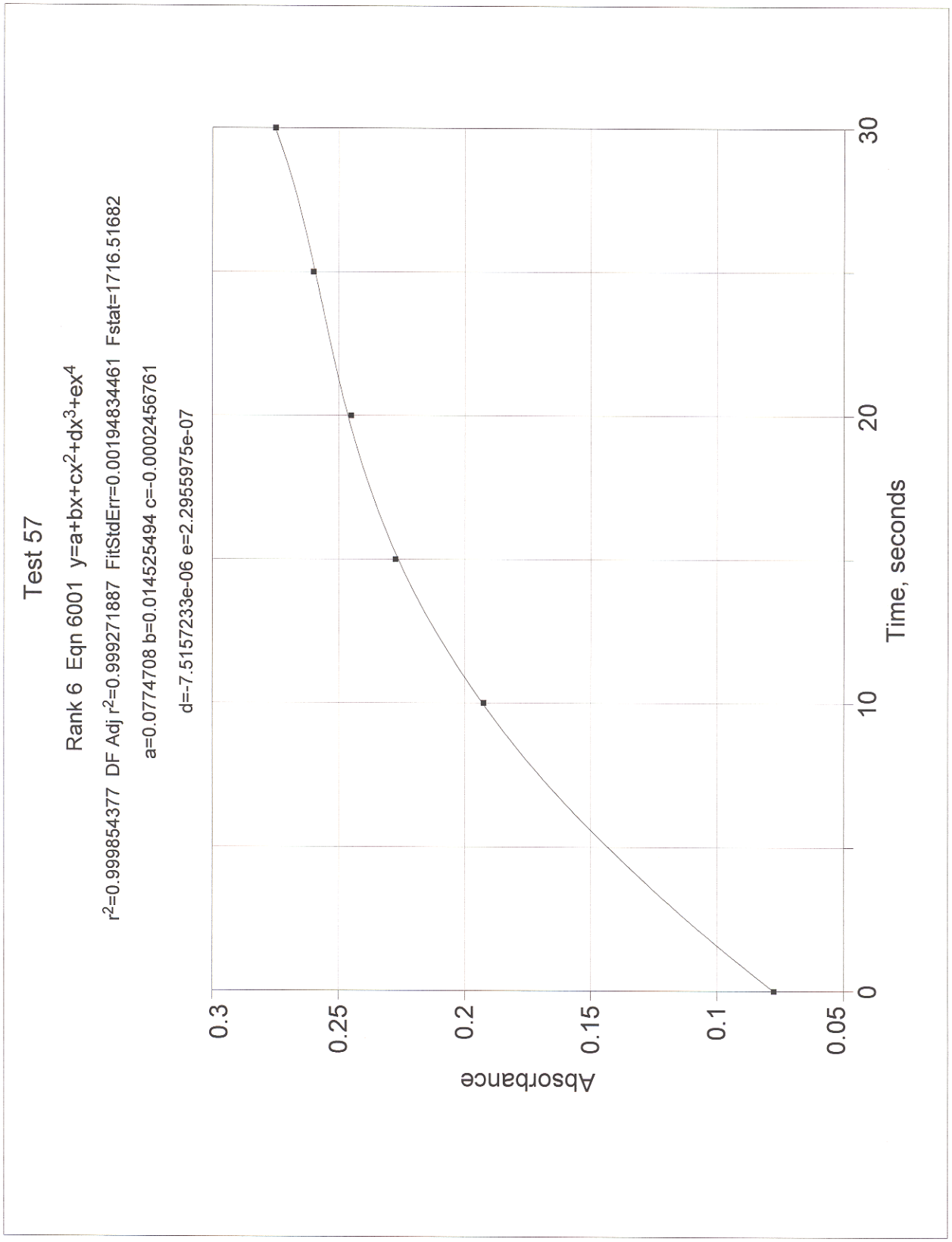

Appendix B: TableCurve Data Files (con't)

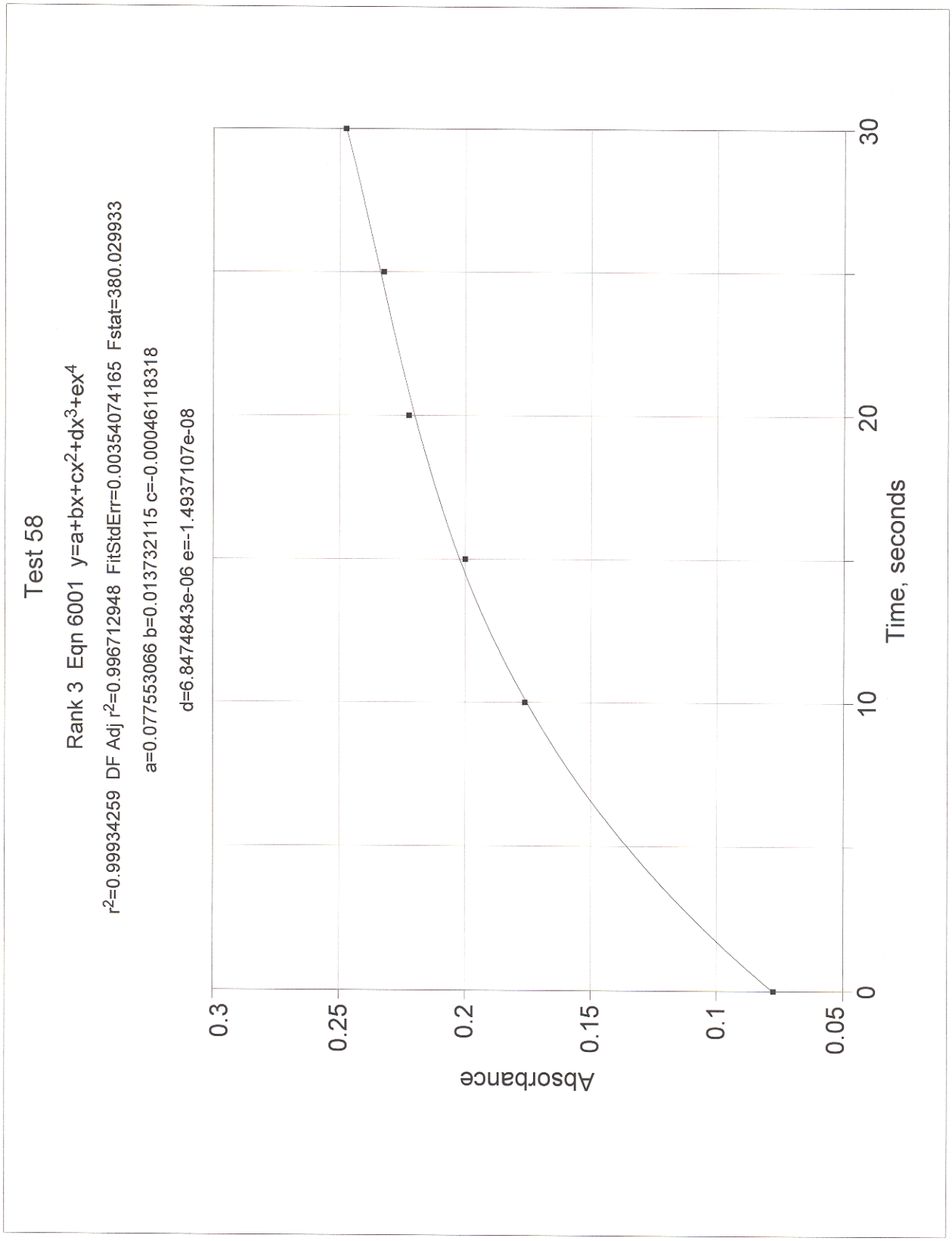

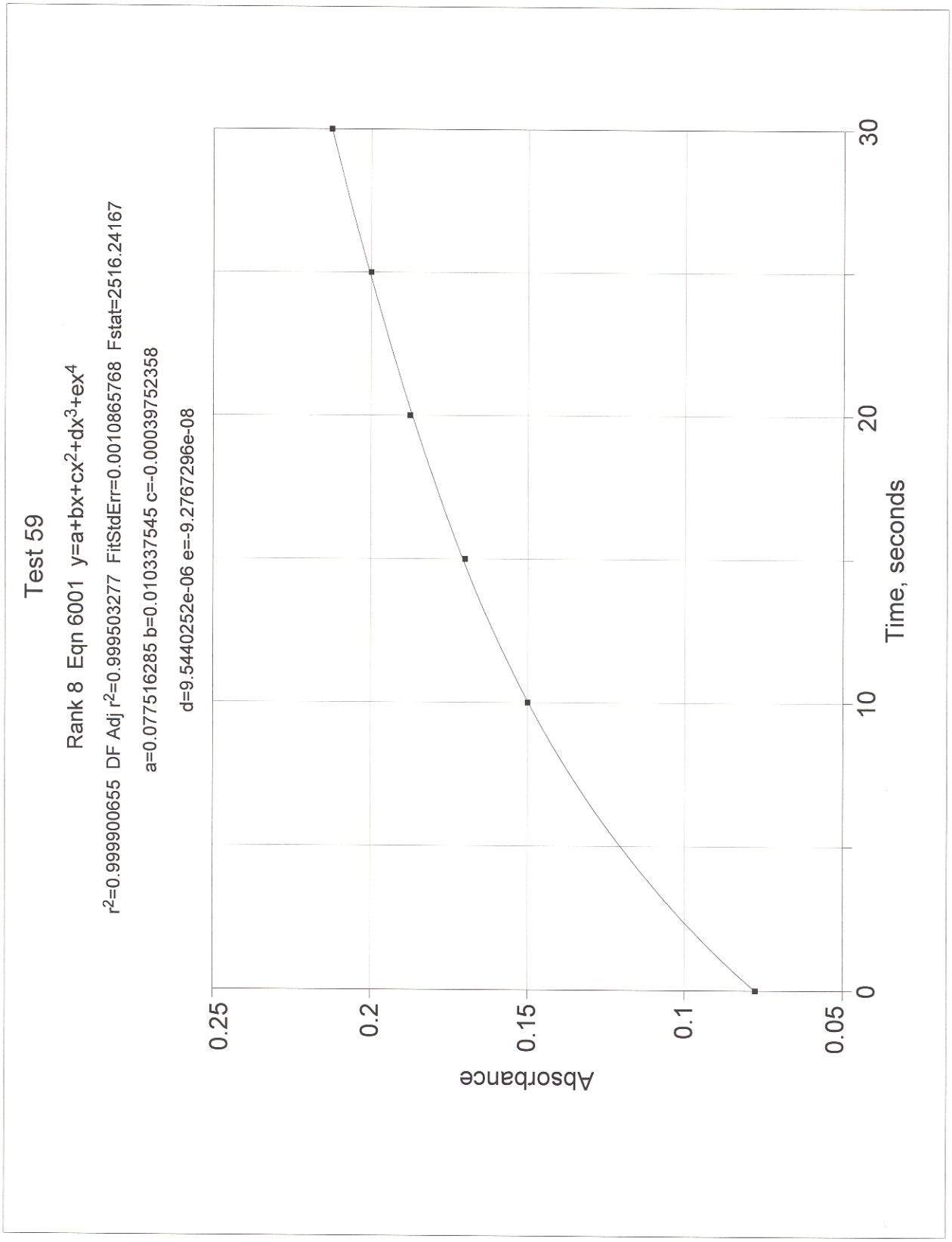
Test 59
Rank 8 Eqn 6001 y=a+bx+cx²+dx³+ex⁴
r²=0.999900655 DF Adj r²=0.999503277 FitStdErr=0.0010865768 Fstat=2516.24167
a=0.077516285 b=0.010337545 c=-0.00039752358
d=9.5440252e-06 e=-9.2767296e-08
Absorbance
0.25
0.2
0.15
0.1
0.05
0
10
20
30
Time, seconds

Appendix B: TableCurve Data Files (con't)

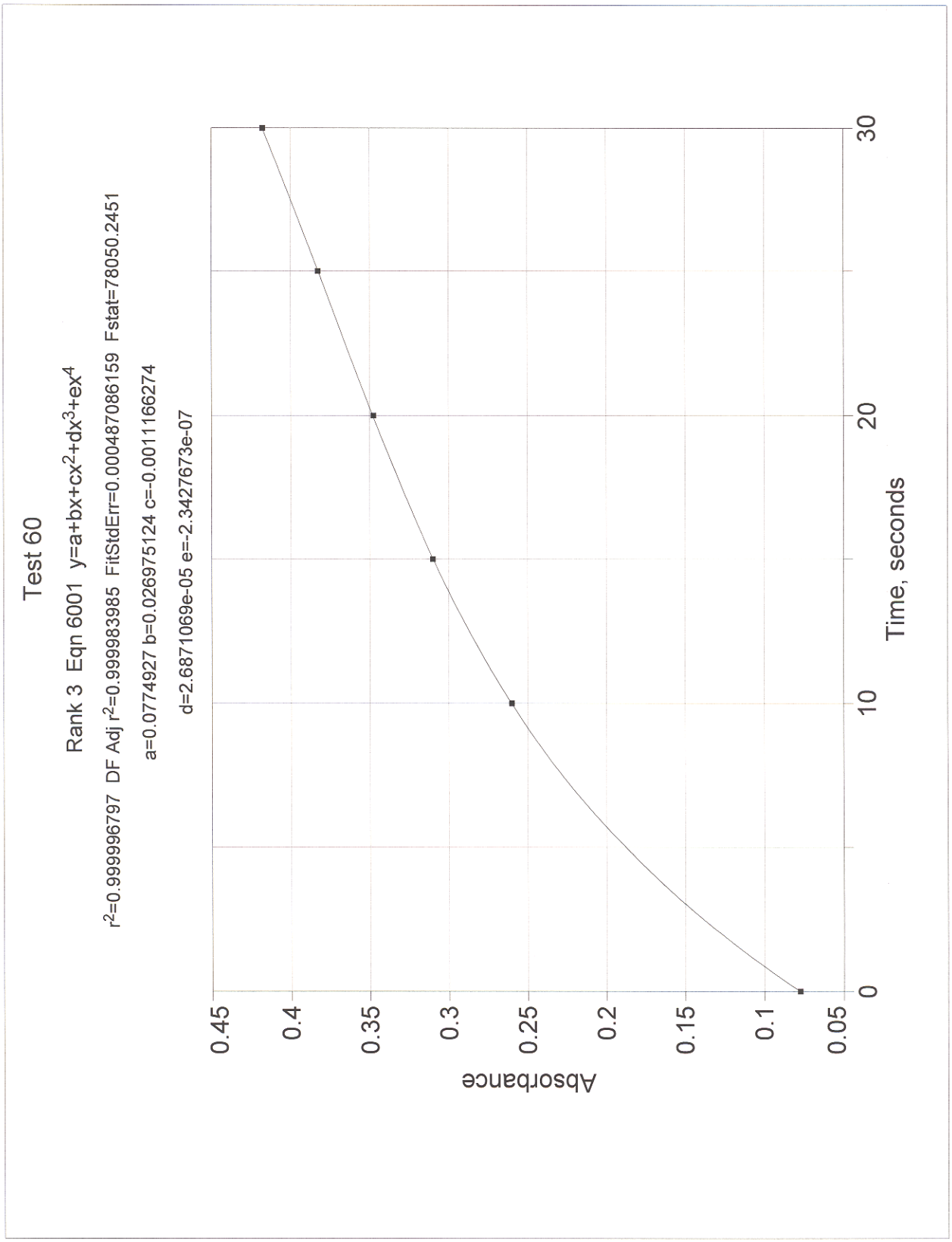

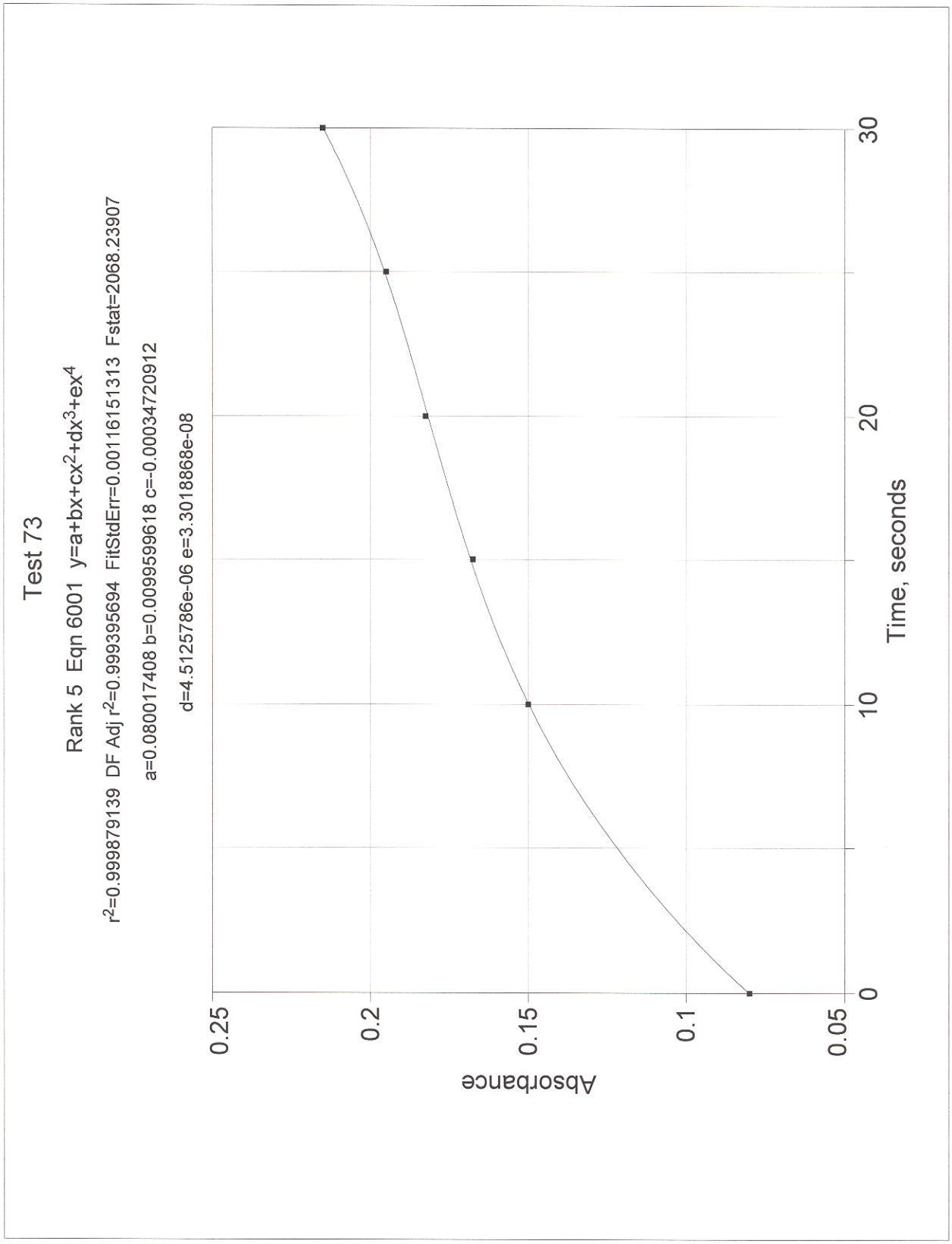
Test 73
Rank 5 Eqn 6001 y=a+bx+cx²+dx³+ex⁴
r²=0.999879139 DF Adj r²=0.999395694 FitStdErr=0.00116151313 Fstat=2068.23907
a=0.080017408 b=0.0099599618 c=-0.000347209 12
d=4.5125786e-06 e=3.3018868e-08
Absorbance
0.25
0.2
0.15
0.1
0.05
0
10
20
30
Time, seconds

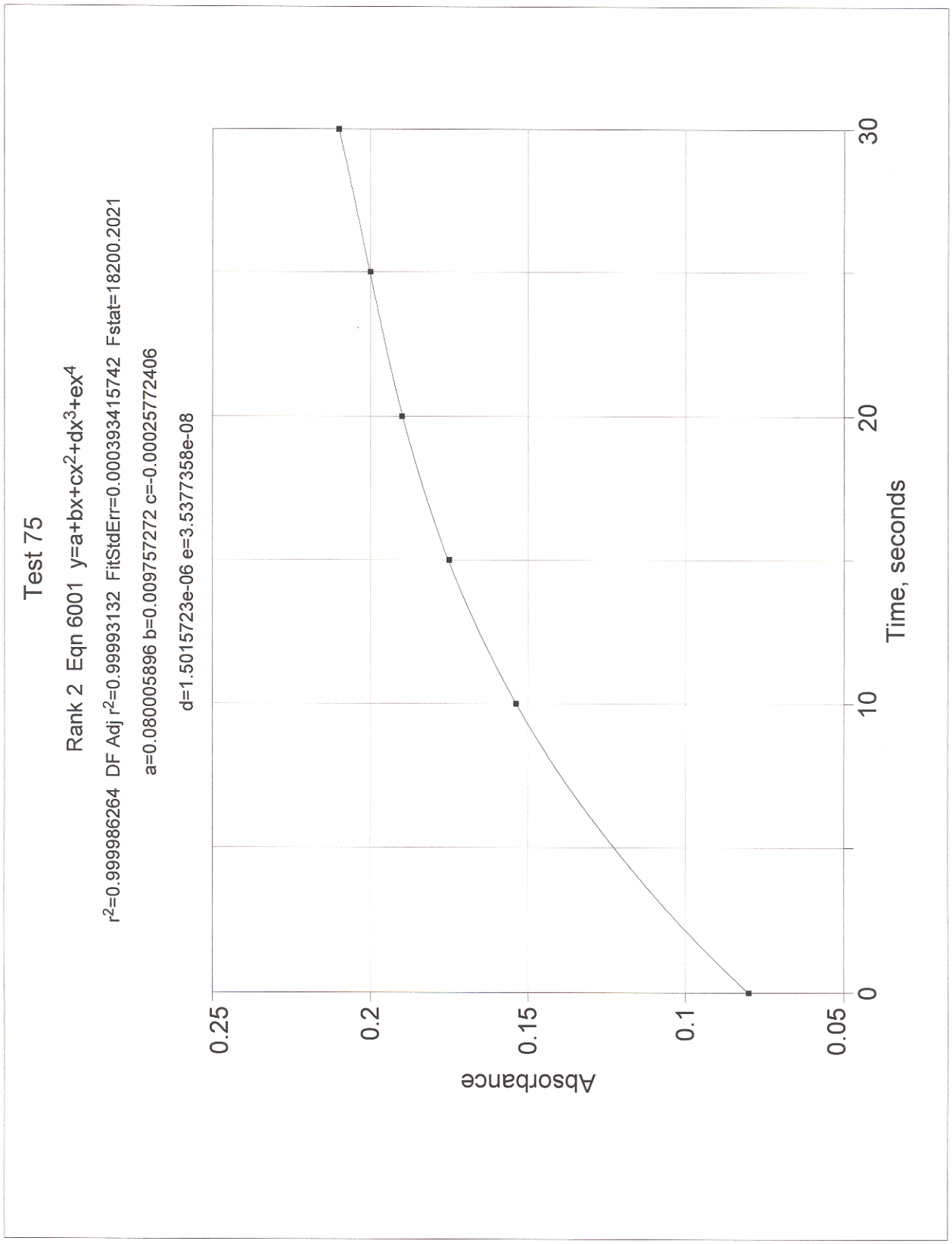
Test 75
Rank 2 Eqn 6001 y=a+bx+cx²+dx³+ex⁴
r²=0.999986264 DF Adj r²=0.99993132 FitStdErr=0.000393415742 Fstat=18200.2021
a=0.080005896 b=0.009757272 c=-0.000257724 06
d=1.5015723e-06 e=3.5377358e-08
Absorbance
0.25
0.2
0.15
0.1
0.05
0
10
20
30
Time, seconds

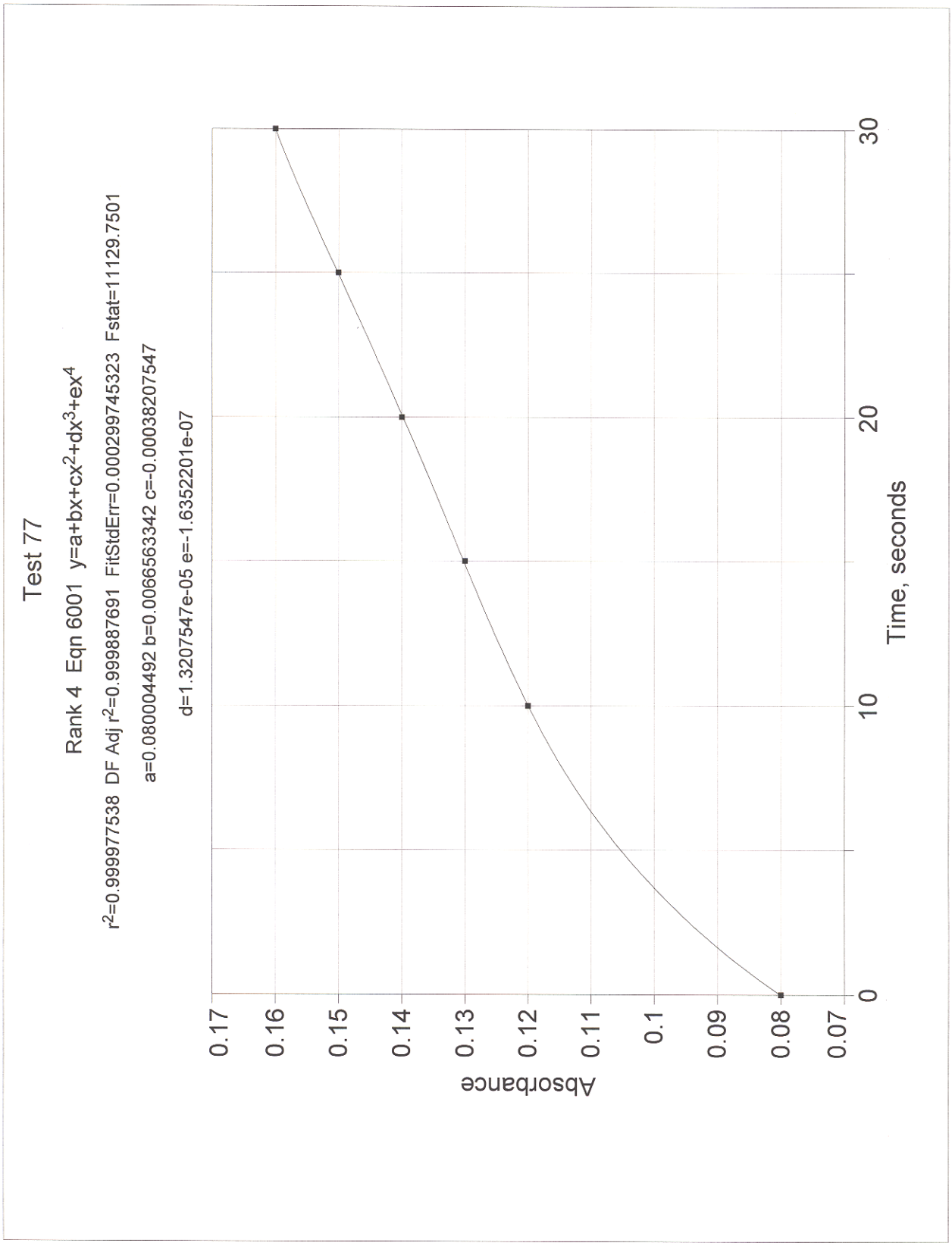
Test 77
Rank 4 Eqn 6001 y=a+bx+cx²+dx³+ex⁴
r²=0.999977538 DF Adj r²=0.999887691 FitStdErr=0.000299745323 Fstat=11129.7501
a=0.080004492 b=0.0066563342 c=-0.00038207547
d=1.3207547e-05 e=-1.6352201e-07
Absorbance
0.17
0.16
0.15
0.14
0.13
0.12
0.11
0.1
0.09
0.08
0.07
0
10
20
30
Time, seconds

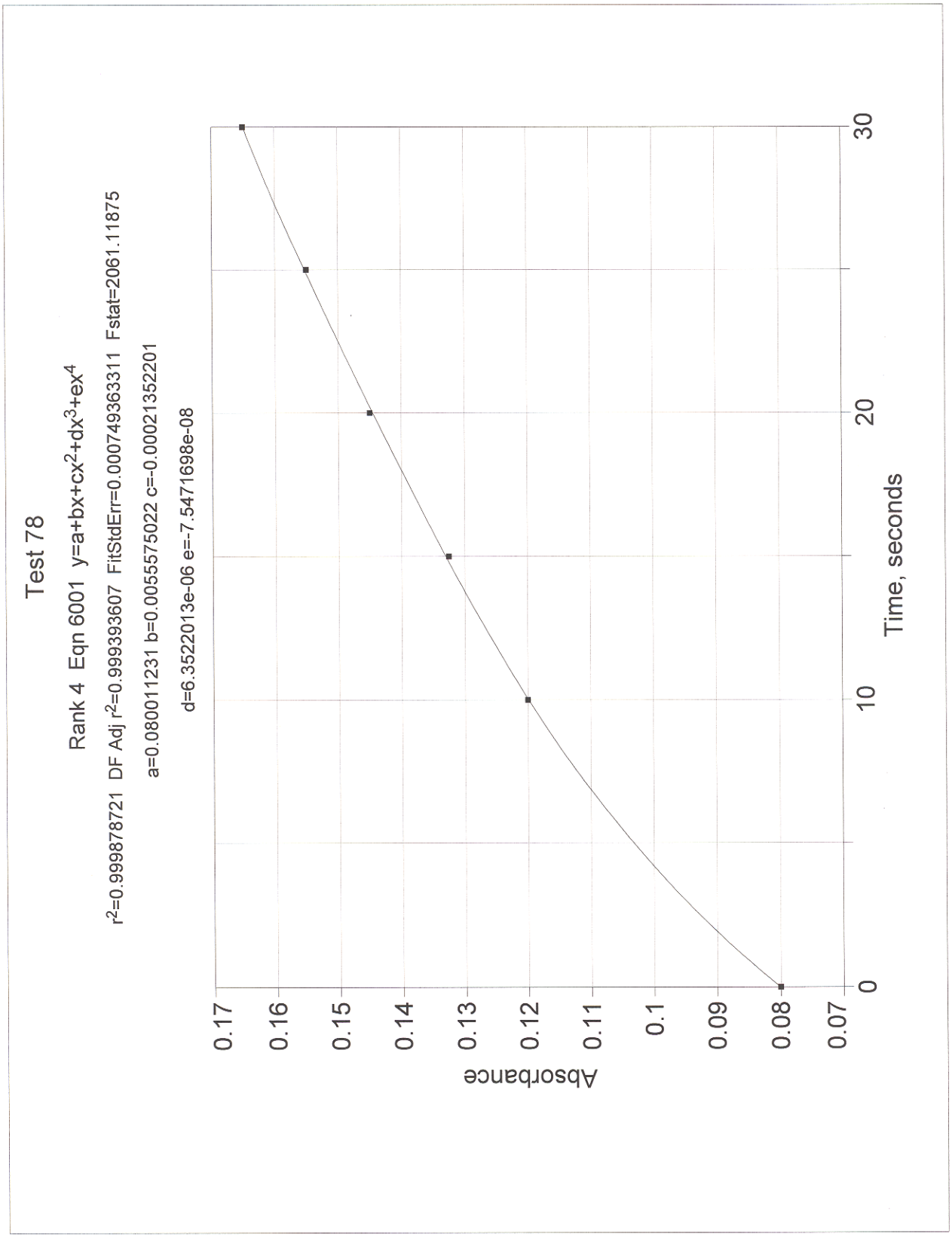
Test 78
Rank 4 Eqn 6001 y=a+bx+cx²+dx³+ex⁴
r²=0.999878721 DF Adj r²=0.999393607 FitStdErr=0.000749363311 Fstat=2061.11875
a=0.080011231 b=0.0055575022 c=-0.00021352201
d=6.3522013e-06 e=-7.5471698e-08
Absorbance
0.17
0.16
0.15
0.14
0.13
0.12
0.11
0.1
0.09
0.08
0.07
0
10
20
30
Time, seconds

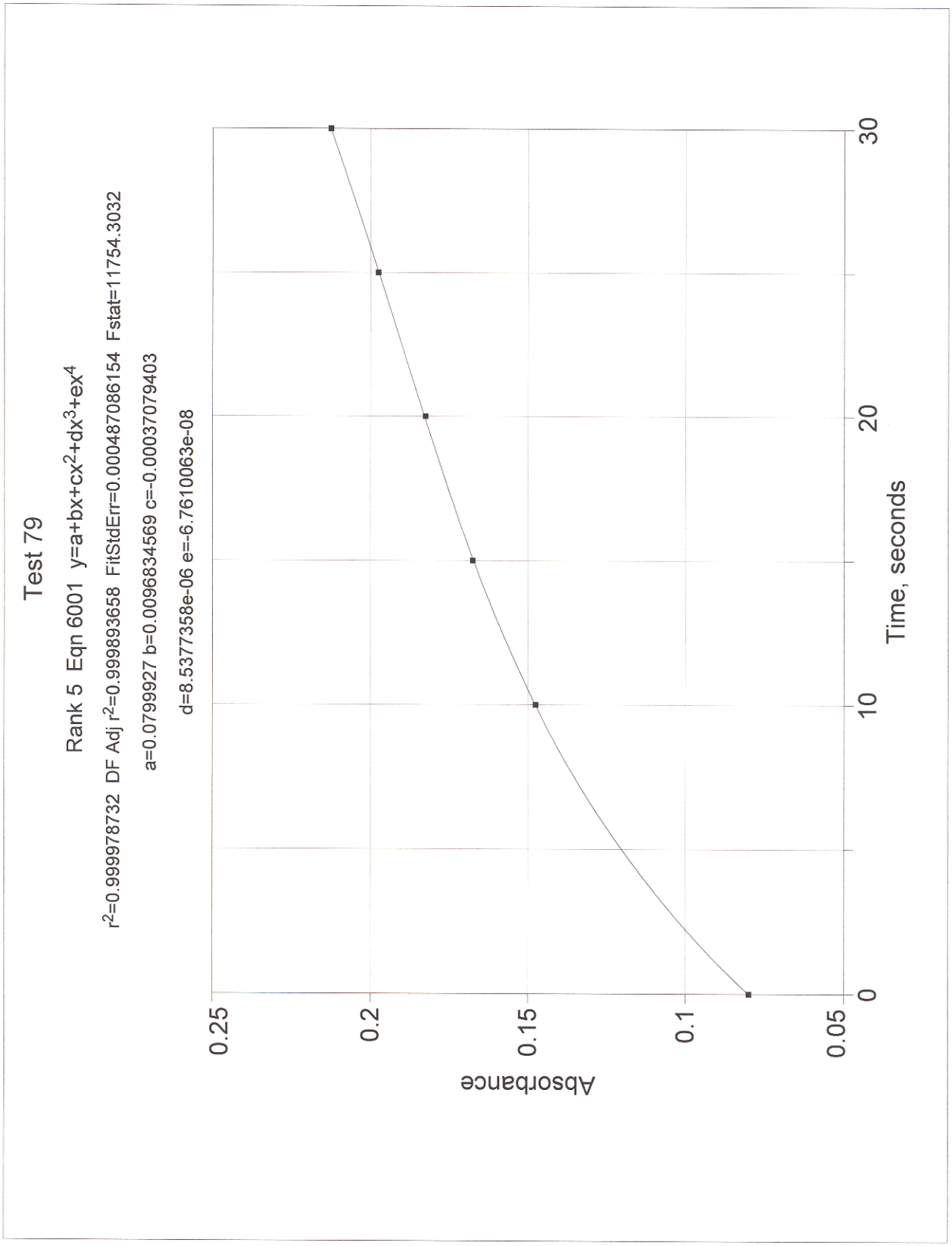
Test 79
Rank 5 Eqn 6001 y=a+bx+cx²+dx³+ex⁴
r²=0.999978732 DF Adj r²=0.999893658 FitStdErr=0.000487086154 Fstat=11754.3032
a=0.0799927 b=0.0096834569 c=-0.00037079403
d=8.5377358e-06 e=-6.7610063e-08
Absorbance
0.25
0.2
0.15
0.1
0.05
0
10
20
30
Time, seconds

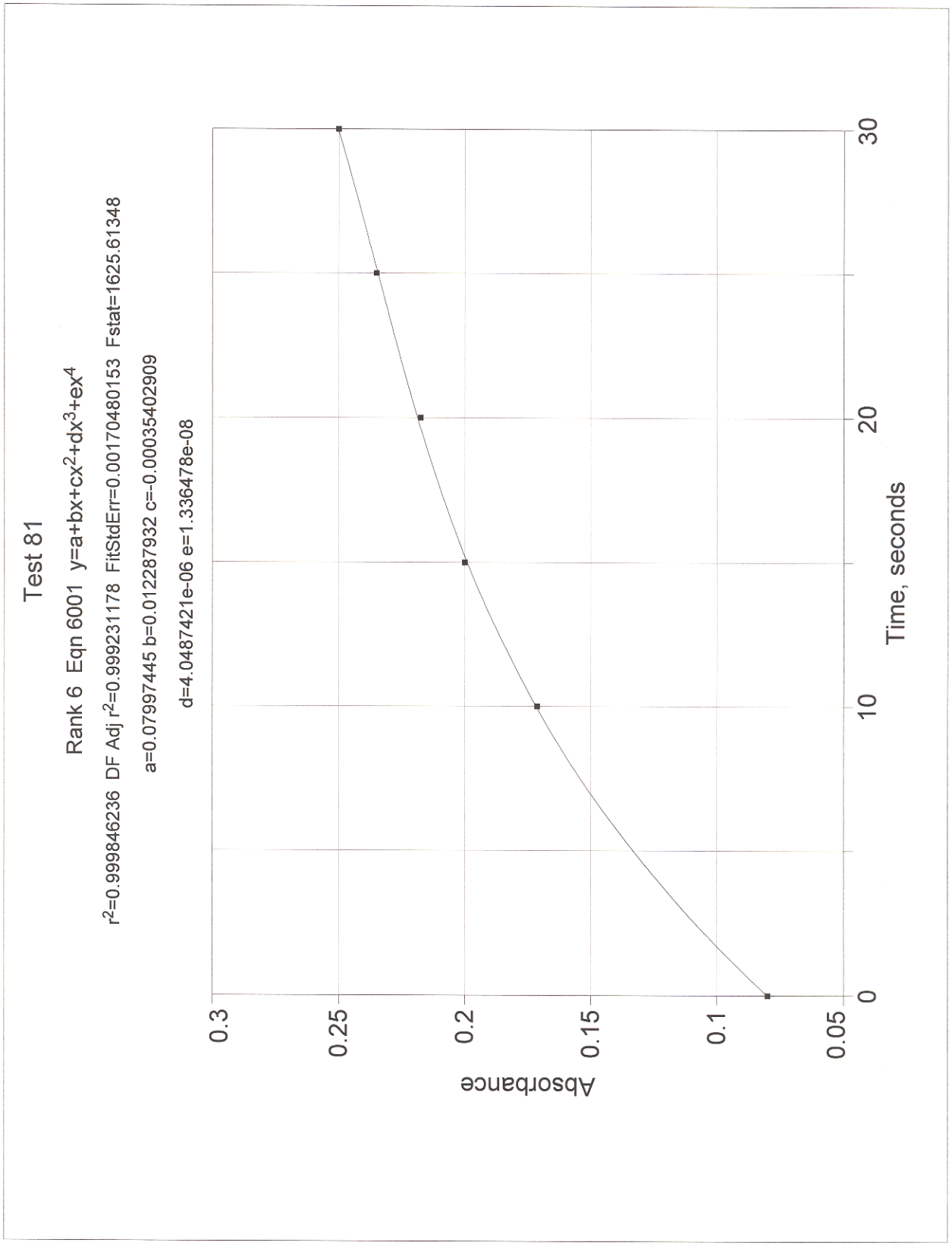
Test 81
Rank 6 Eqn 6001 y=a+bx+cx²+dx³+ex⁴
r²=0.999846236 DF Adj r²=0.999231178 FitStdErr=0.00170480153 Fstat=1625.61348
a=0.07997445 b=0.012287932 c=-0.000354029 09
d=4.0487421e-06 e=1.336478e-08
Absorbance
0.3
0.25
0.2
0.15
0.1
0.05
0
10
20
30
Time, seconds

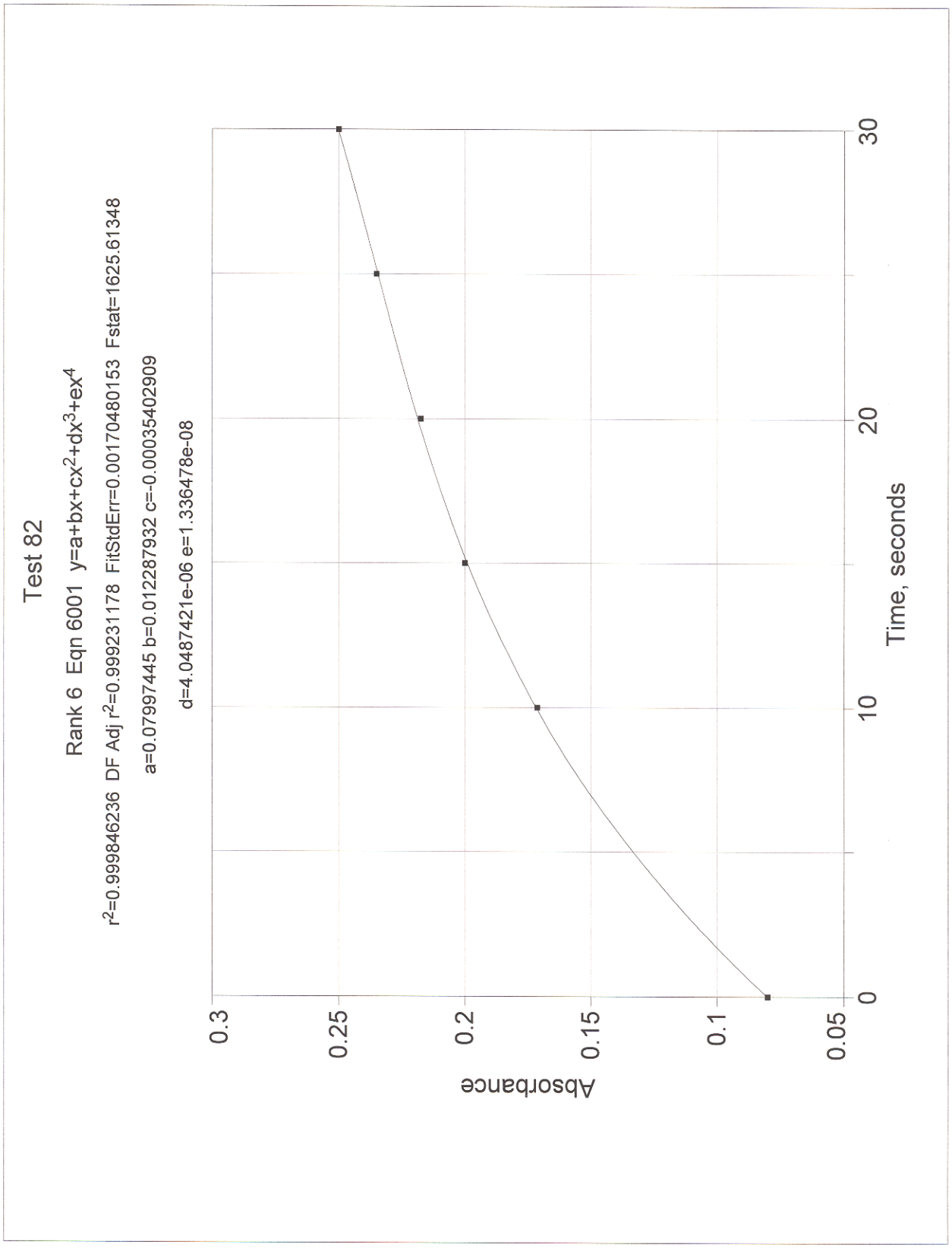
Test 82
Rank 6 Eqn 6001 y=a+bx+cx²+dx³+ex⁴
r²=0.999846236 DF Adj r²=0.999231178 FitStdErr=0.00170480153 Fstat=1625.61348
a=0.07997445 b=0.012287932 c=-0.00035402909
d=4.0487421e-06 e=1.336478e-08
Absorbance
0.3
0.25
0.2
0.15
0.1
0.05
0
10
20
30
Time, seconds

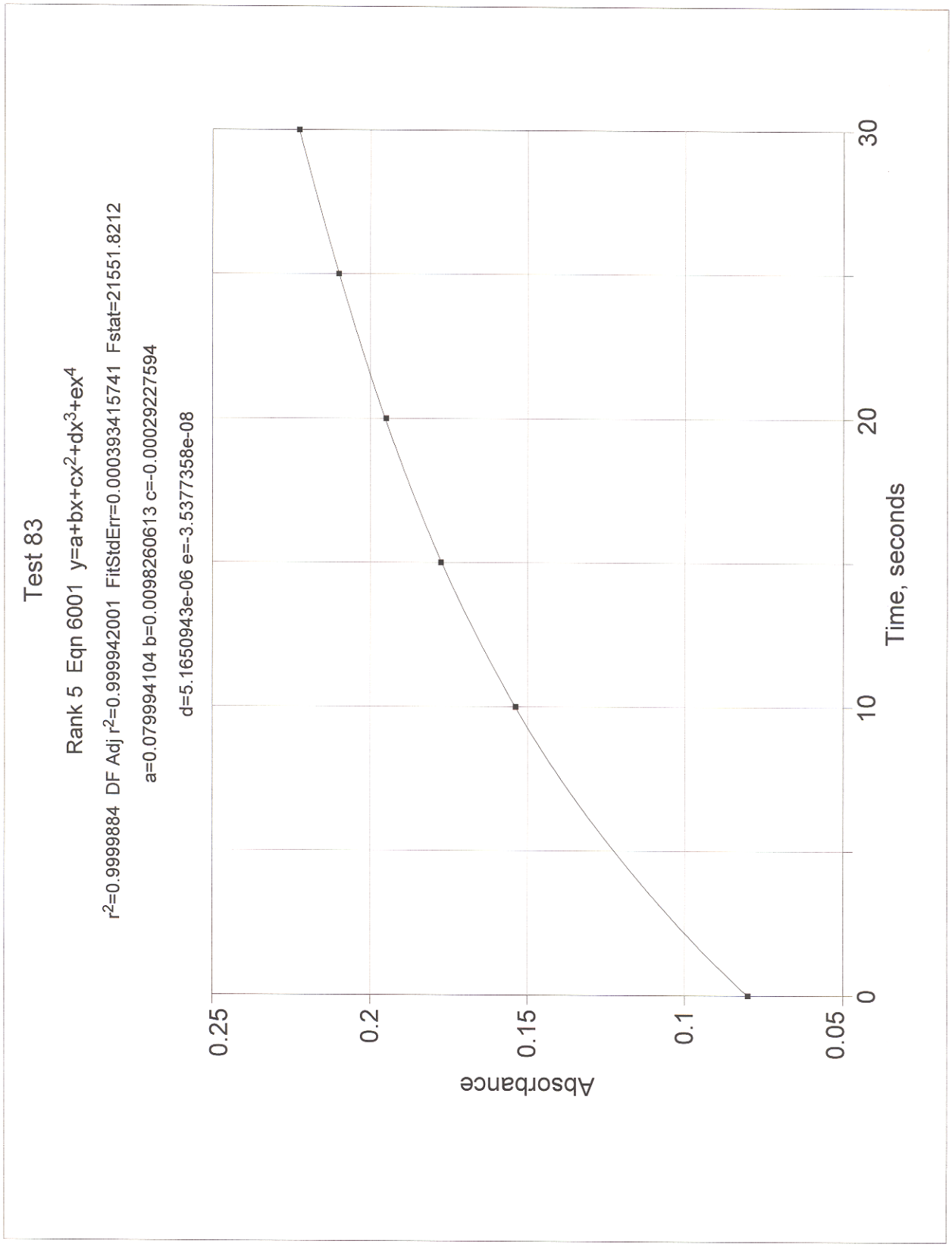
Test 83
Rank 5 Eqn 6001 y=a+bx+cx²+dx³+ex⁴
r²=0.9999884 DF Adj r²=0.9999942001 FitStdErr=0.0003934157 41 Fstat=21551.8212
a=0.0799941 04 b=0.0098260613 c=-0.00029227594
d=5.1650943e-06 e=-3.5377358e-08
Absorbance
0.25
0.2
0.15
0.1
0.05
0
10
20
30
Time, seconds

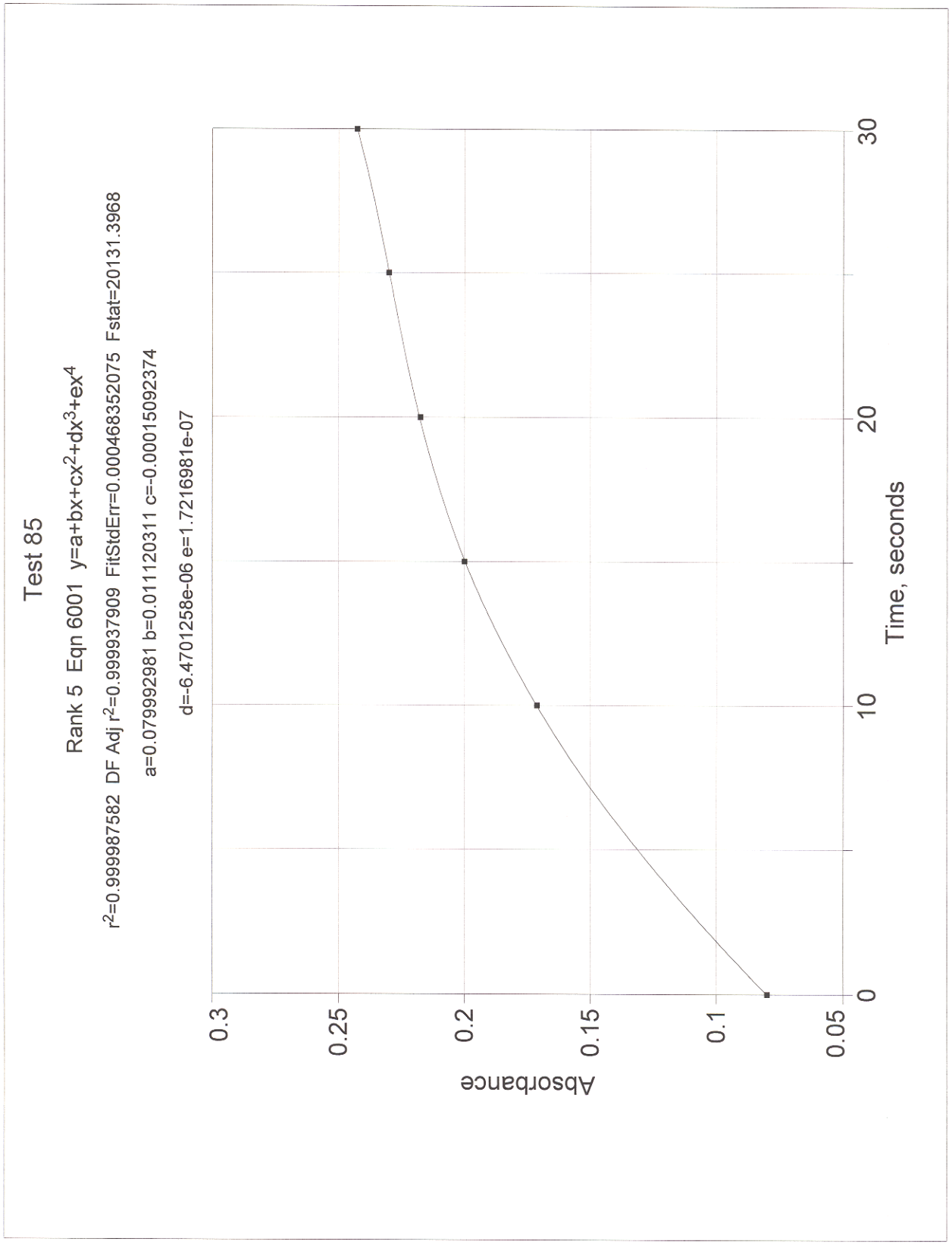
Test 85
Rank 5 Eqn 6001 y=a+bx+cx²+dx³+ex⁴
r²=0.999987582 DF Adj r²=0.999937909 FitStdErr=0.000468352075 Fstat=20131.3968
a=0.079992981 b=0.011120311 c=-0.00015092374
d=-6.4701258e-06 e=1.7216981e-07
Absorbance
0.3
0.25
0.2
0.15
0.1
0.05
0
10
20
30
Time, seconds

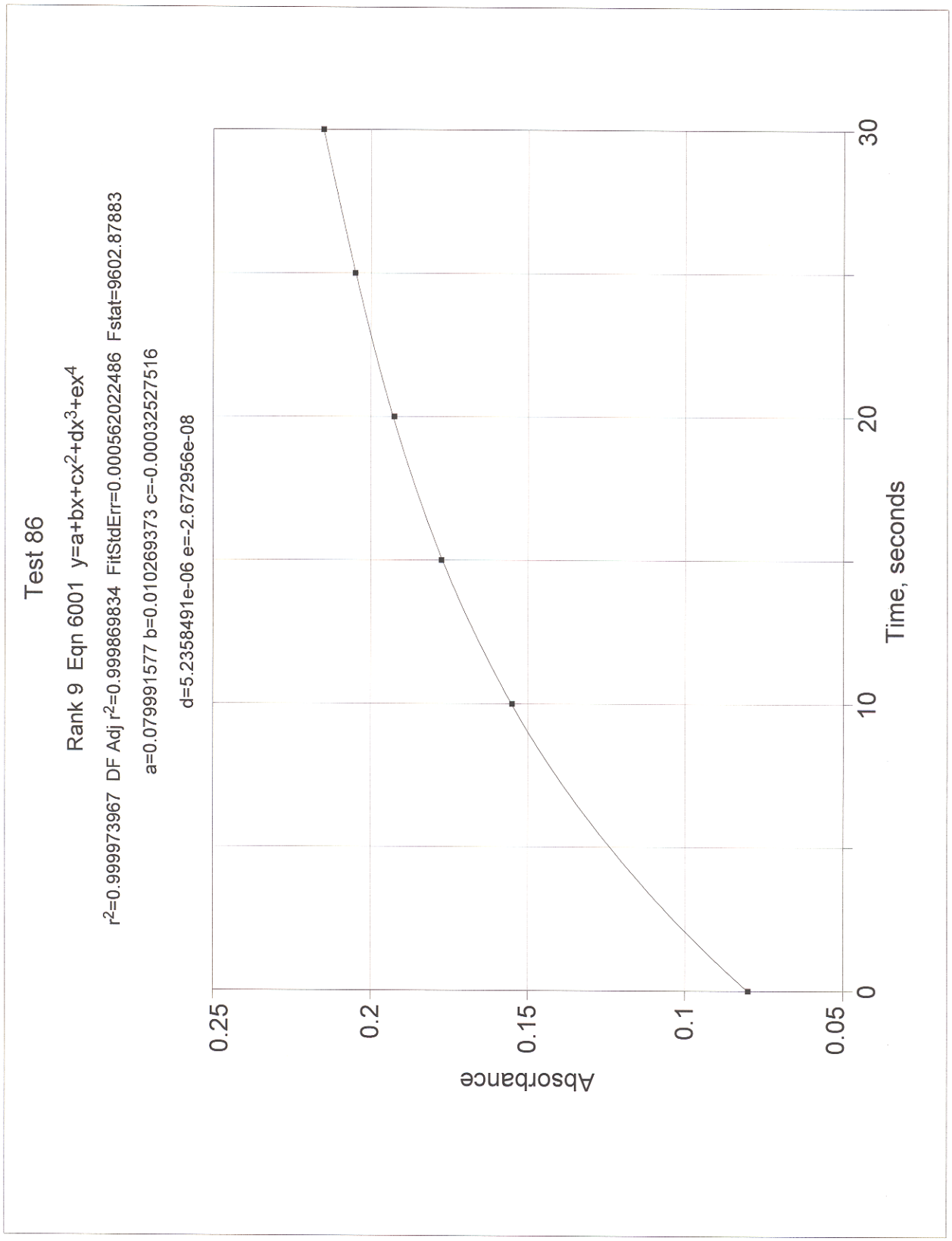
Test 86
Rank 9 Eqn 6001 y=a+bx+cx²+dx³+ex⁴
r²=0.999973967 DF Adj r²=0.999869834 FitStdErr=0.000562022486 Fstat=9602.87883
a=0.079991577 b=0.010269373 c=-0.00032527516
d=5.2358491e-06 e=-2.672956e-08
Absorbance
0.25
0.2
0.15
0.1
0.05
0
10
20
30
Time, seconds

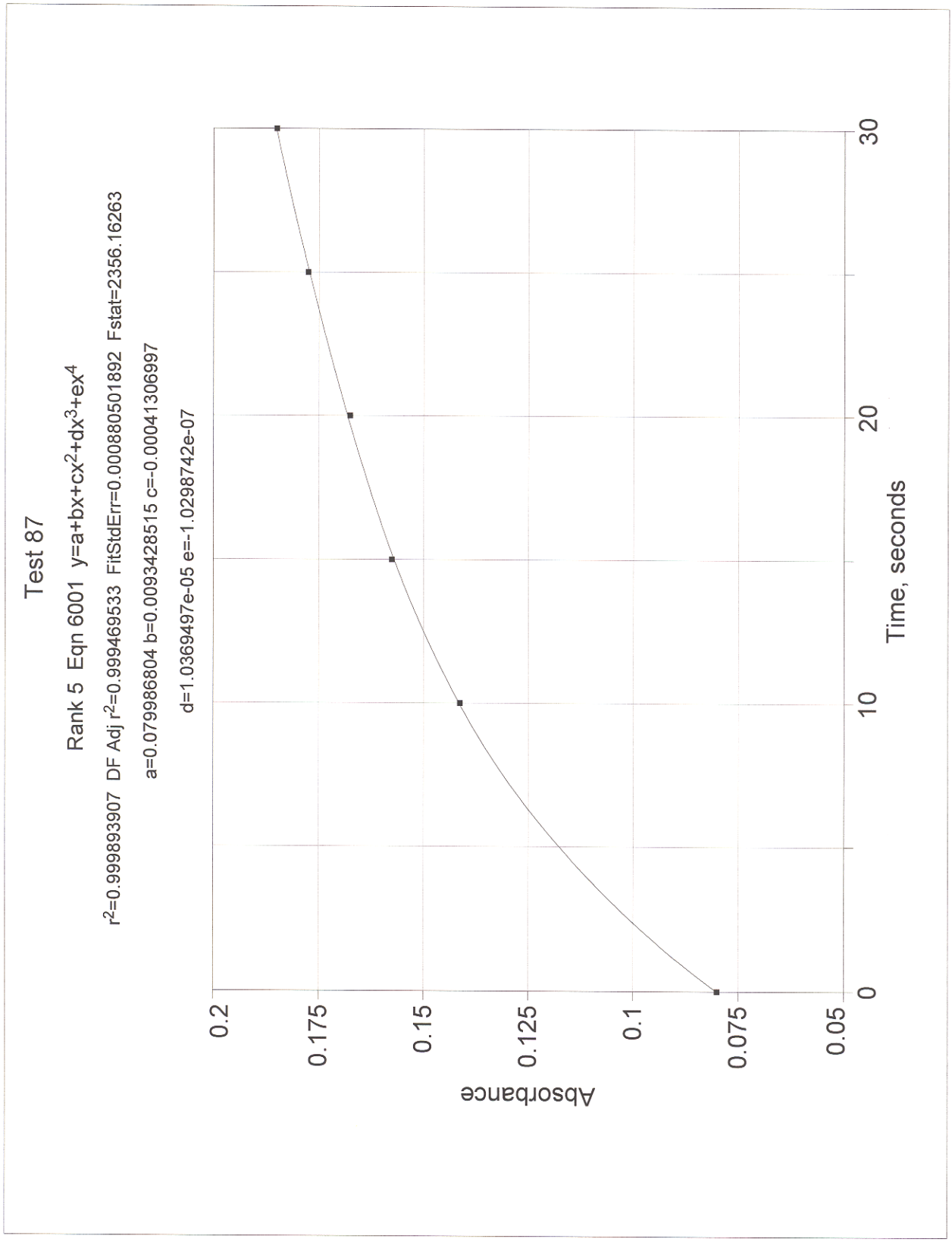
Test 87
Rank 5 Eqn 6001 y=a+bx+cx²+dx³+ex⁴
r²=0.999893907 DF Adj r²=0.999469533 FitStdErr=0.000880501892 Fstat=2356.16263
a=0.079986804 b=0.0093428515 c=-0.00041306997
d=1.0369497e-05 e=-1.0298742e-07
Absorbance
0.2
0.175
0.15
0.125
0.1
0.075
0.05
0
10
20
30
Time, seconds

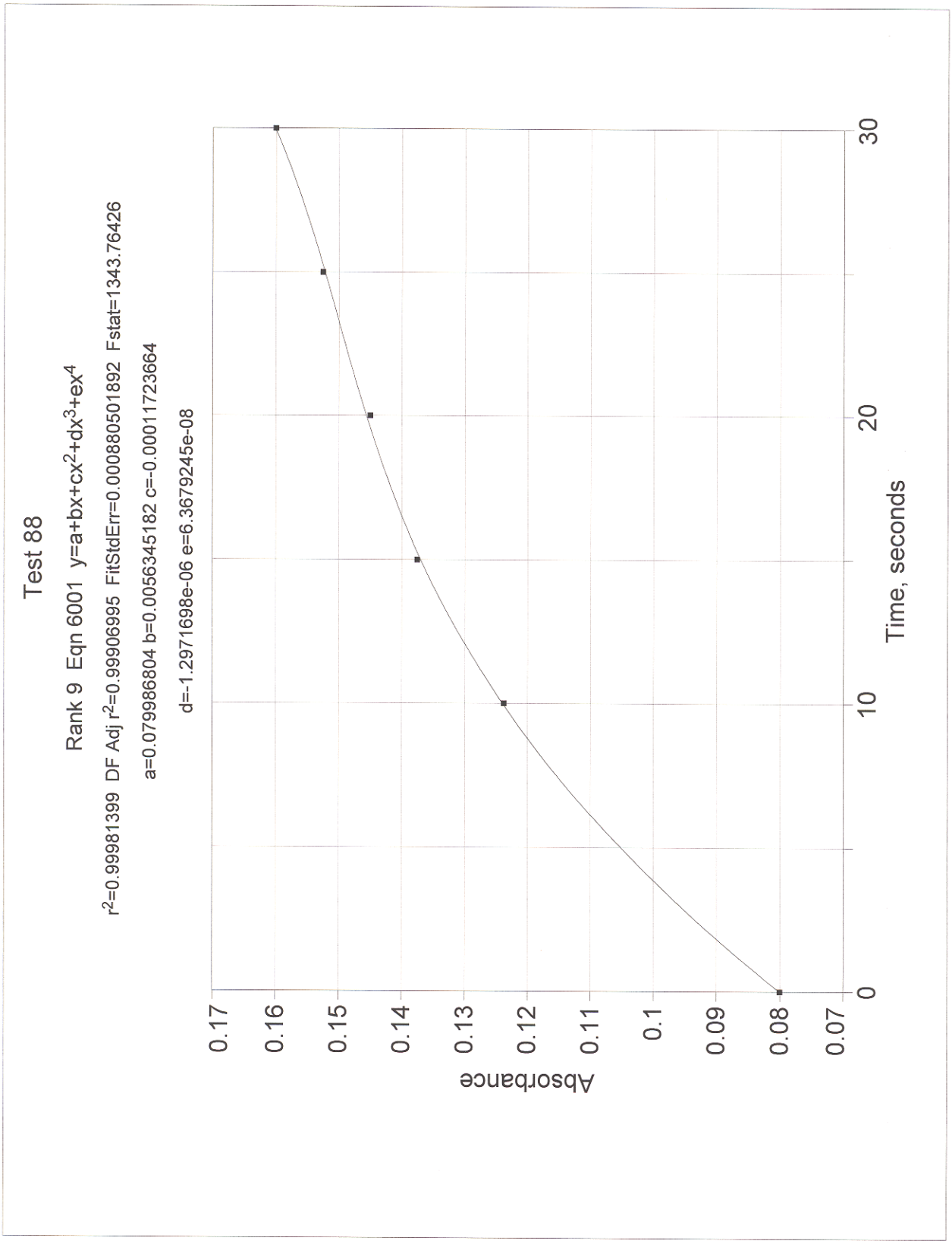
Test 88
Rank 9 Eqn 6001 y=a+bx+cx²+dx³+ex⁴
r²=0.99981399 DF Adj r²=0.99906995 FitStdErr=0.000880501892 Fstat=1343.76426
a=0.079986804 b=0.0056345182 c=-0.00011723664
d=-1.2971698e-06 e=6.3679245e-08
Absorbance
0.17
0.16
0.15
0.14
0.13
0.12
0.11
0.1
0.09
0.08
0.07
0
10
20
30
Time, seconds

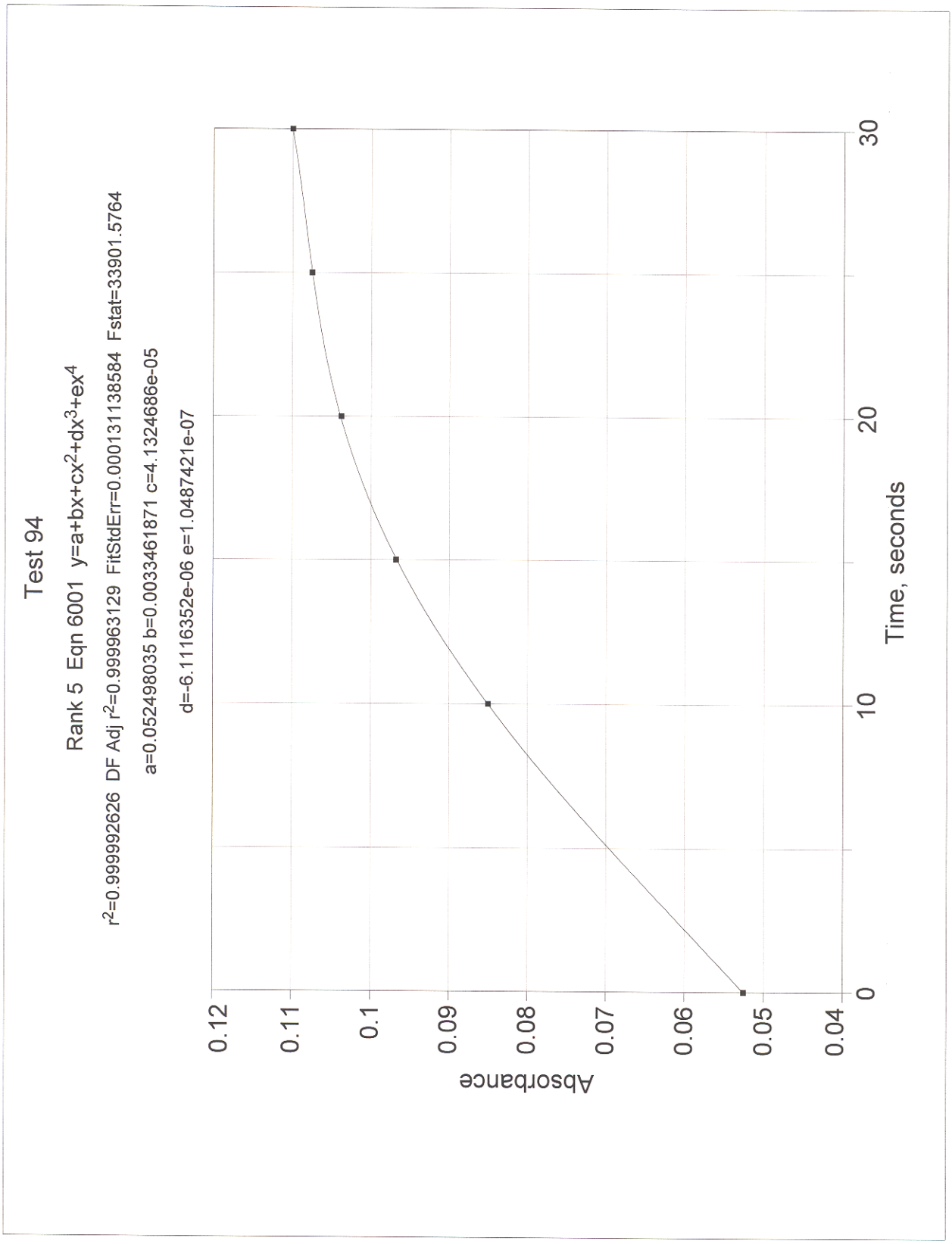
Test 94
Rank 5 Eqn 6001 y=a+bx+cx²+dx³+ex⁴
r²=0.999992626 DF Adj r²=0.999963129 FitStdErr=0.000131138584 Fstat=33901.5764
a=0.052498035 b=0.0033461871 c=4.1324686e-05
d=-6.1116352e-06 e=1.0487421e-07
Absorbance
0.12
0.11
0.1
0.09
0.08
0.07
0.06
0.05
0.04
0
10
20
30
Time, seconds

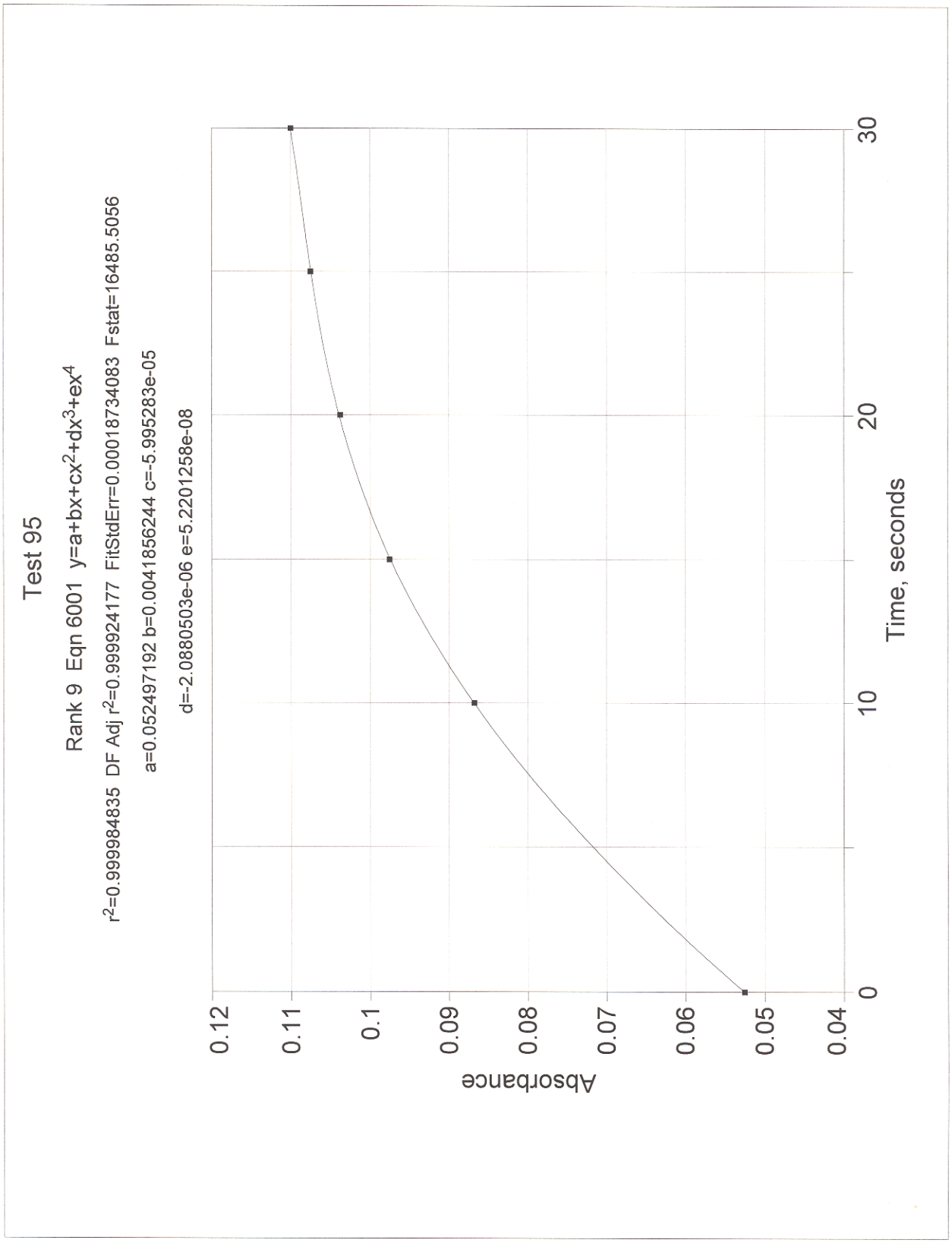
Test 95
Rank 9 Eqn 6001 y=a+bx+cx²+dx³+ex⁴
r²=0.999984835 DF Adj r²=0.999924177 FitStdErr=0.00018734083 Fstat=16485.5056
a=0.052497192 b=0.0041856244 c=-5.995283e-05
d=-2.0880503e-06 e=5.2201258e-08
Absorbance
0.12
0.11
0.1
0.09
0.08
0.07
0.06
0.05
0.04
0
10
20
30
Time, seconds

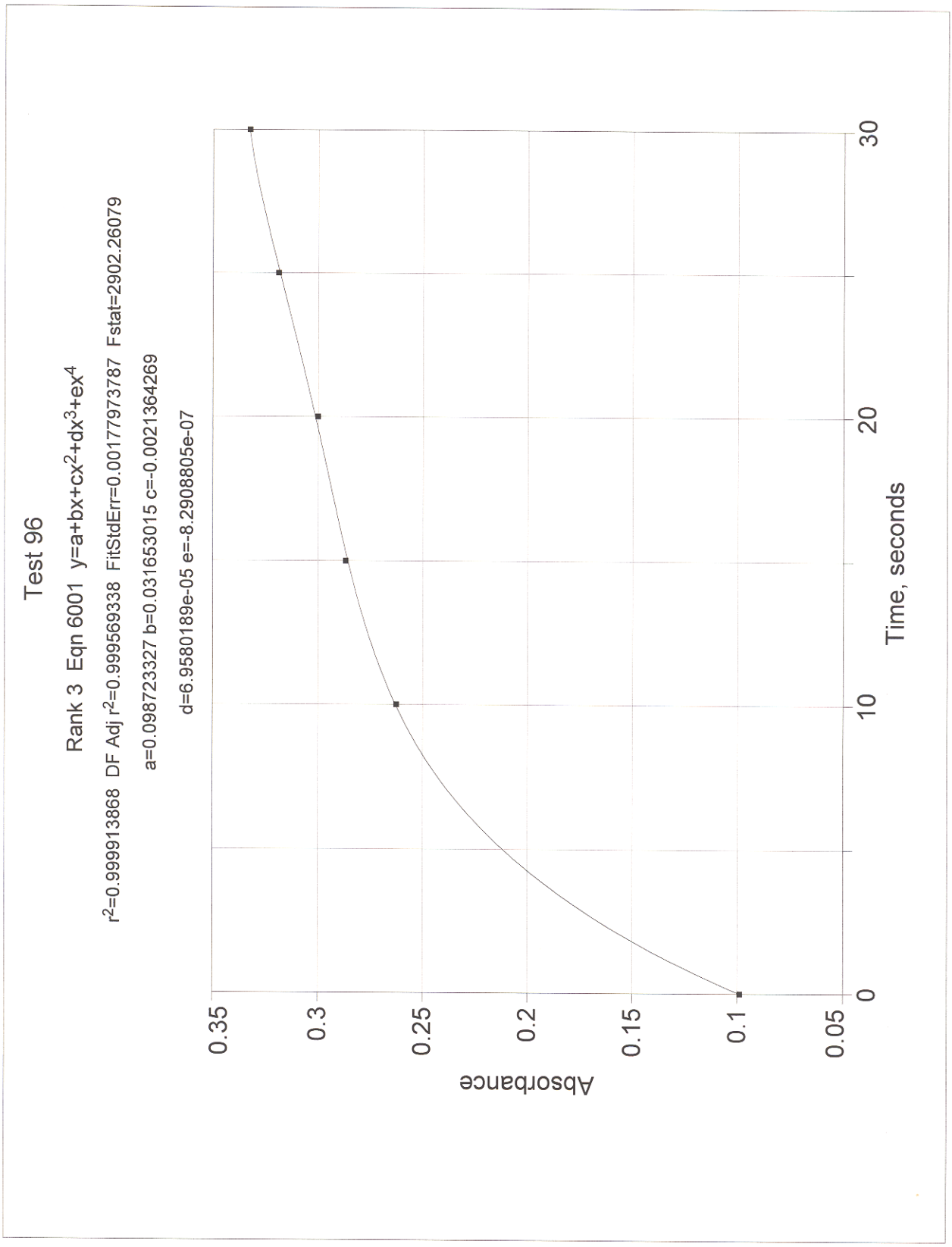
Test 96
Rank 3 Eqn 6001 y=a+bx+cx²+dx³+ex⁴
r²=0.999913868 DF Adj r²=0.999569338 FitStdErr=0.00177973787 Fstat=2902.26079
a=0.098723327 b=0.031653015 c=-0.0021364269
d=6.9580189e-05 e=-8.2908805e-07
Absorbance
0.35
0.3
0.25
0.2
0.15
0.1
0.05
0
10
20
30
Time, seconds

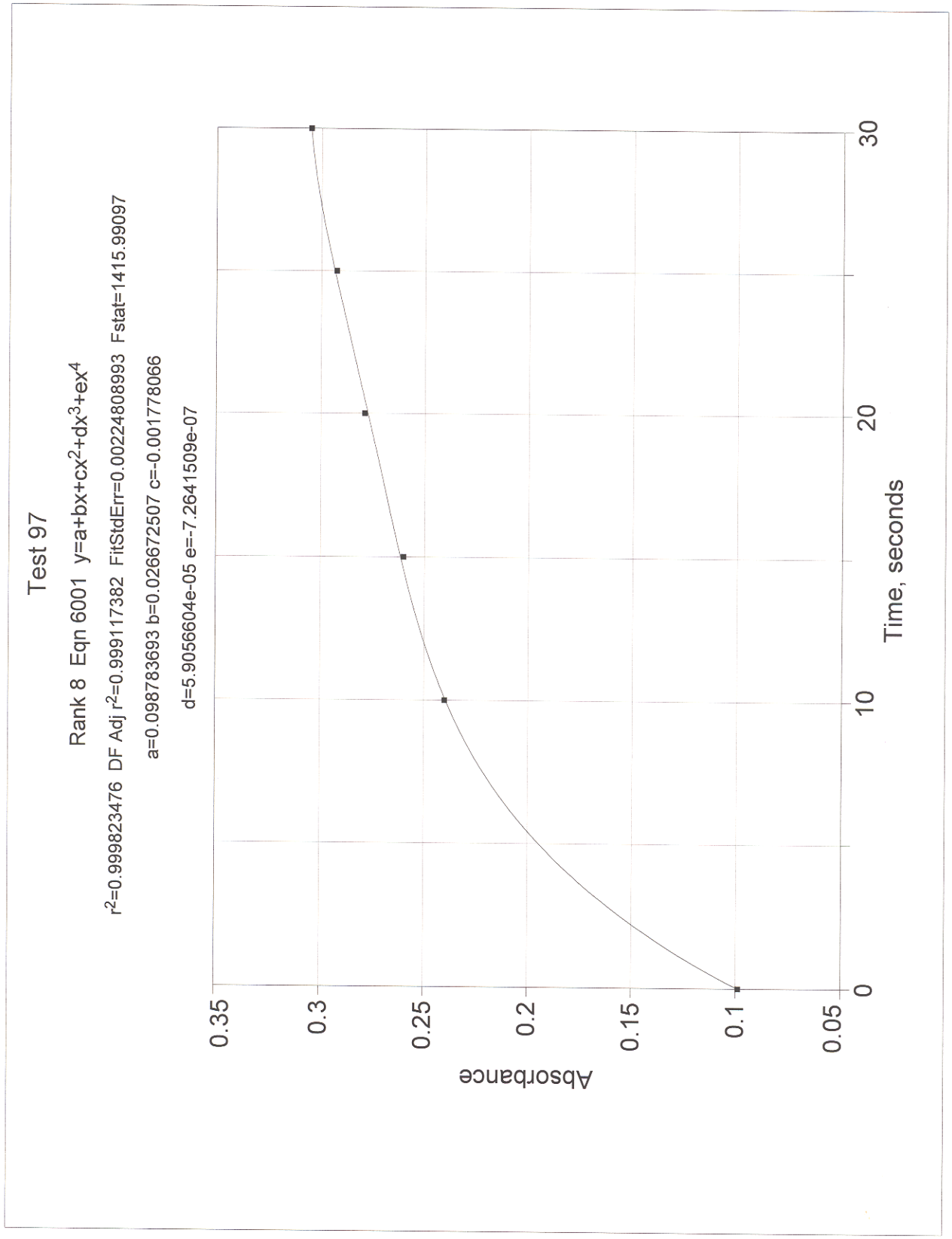
Test 97
Rank 8 Eqn 6001 y=a+bx+cx²+dx³+ex⁴
r²=0.999823476 DF Adj r²=0.999117382 FitStdErr=0.00224808993 Fstat=1415.99097
a=0.098783693 b=0.026672507 c=-0.001778066
d=5.9056604e-05 e=-7.2641509e-07
Absorbance
0.35
0.3
0.25
0.2
0.15
0.1
0.05
0
10
20
30
Time, seconds

VITA

JOHN D. DAVIS, JR.

Personal Data:	Date of Birth: May 27, 1962
	Place of Birth: Georgetown, Kentucky
	Marital Status: Single
Education:	Desoto High School, Arcadia, Florida
	Milligan College, Elizabethton, Tennessee; Chemistry, B. S., 1984
	East Tennessee State University, Johnson City, Tennessee; Chemistry, M. S., 2003
Professional Experience:	Chemist and Production Manager, Hanes Dye and Finishing Co., Winston-Salem, North Carolina, 1984 – 1988.
	Production Supervisor, Beecham Pharmaceuticals, Bristol, Tennessee, 1988 – 1989.
	Chemist and Laboratory Manager, Nuclear Fuel Services, Erwin, Tennessee, 1989 – Present
Patents:	"Metal and Fluorine Values Recovery From Fluoride Salt Matrices", Patent No. 5,881,359, March 9, 1999.
Trade Secrets:	"Mercury Mixed-Waste Treatment Technology", Nuclear Fuel Services, 1994.

"Mixed-Waste Sediment Treatment Technology", Nuclear Fuel Services, 1995.

"Recovery of Uranium and Antimony Values from Spent Oxide Catalysts", Nuclear Fuel Services, 1997.

"Destruction of Semi-Volatile Hazardous Organic Compounds by a Novel Chemical Wet-Oxidation Process", Nuclear Fuel Services, 1998.